CHALMERS
UNIVERSITY OF TECHNOLOGY

Sustainable Manufacturing: Metal Cutting Fluid – From Mineral Oil to Vegetable Oil

Master's thesis in Materials Science

Roman Kalkavan

Department of Industrial and Materials Science
CHALMERS UNIVERSITY OF TECHNOLOGY
Gothenburg, Sweden 2019

Master's thesis 2019

Sustainable Manufacturing: Metal Cutting Fluid – From Mineral Oil to Vegetable Oil

by

ROMAN KALKAVAN

CHALMERS
UNIVERSITY OF TECHNOLOGY

Department of Industrial and Materials Science
Division of Materials and Manufacturing
Chalmers University of Technology
Gothenburg, Sweden 2019

Sustainable Manufacturing: Metal Cutting Fluid – From Mineral Oil to Vegetable Oil
ROMAN KALKAVAN

Supervisor: Amir Malakizadi, Department of Industrial and Materials Science
Supervisor: Eric Tam, Department of Industrial and Materials Science

Examiner: Professor Lars Nyborg, Department of Industrial and Materials Science

Master's Thesis 2019:55119
Department of Industrial and Materials Science
Division of Materials and Manufacturing
Chalmers University of Technology
SE-412 96 Gothenburg
Sweden
Telephone +46 31 772 1000

Chalmers Reproservice
Gothenburg, Sweden 2019

Sustainable Manufacturing: Metal Cutting Fluid – From Mineral Oil to Vegetable Oil

ROMAN KALKAVAN

Department of Industrial and Materials Science

Chalmers University of Technology

Abstract

Metal cutting fluids (MCFs) are widely used in industry. This raises the concerns about sustainability, biodegradability and the associated health risks. Numerous studies show the benefits of using vegetable oil-based over mineral oil-based MCFs. Having numerous advantages like lower production cost and lower environmental impact, the vegetable oil-based MCF could become the sustainable alternative for the conventional mineral oils. This thesis work aims to evaluate the performance of four mixtures of neat vegetable and mineral oils in the machining of free-cutting steel (FCS). The work is primarily focused on the tool wear, the surface roughness of the machined components, and the microstructure of the raw materials. The results show no significant difference between the wear mechanisms of the tools, predominant being the adhesion wear. The minimum tool wear on the coated carbide inserts occurred when machining with 100% neat vegetable oil and only slightly increased as the volume percentage of mineral oil in the cutting fluid increased. The surface roughness was not affected by the changes in the cutting fluid. The microscopic analysis revealed that the microstructural components of the free-cutting steel include ferrite and pearlite together with lead (Pb) and manganese sulfide (MnS) inclusions.

Keywords: free-cutting steel, metal cutting fluid, tool wear.

Acknowledgements

I am thankful to my supervisors Amir Malakizadi and Eric Tam for supporting and assisting me throughout my thesis, guiding me towards its completion while also taking care of the organizational matters. I would also like to thank my examiner Professor Lars Nyborg.

I am grateful to all the people who have contributed to this work: Linda Fransson and Jens Ringborg at Gnosjö Automatsvarvning for hosting and providing everything necessary for the practical part; Eva Troell and Johan Berglund at RISE IVF for organizing the project and helping with the interferometry tests; Lennart Samuelsson, Jenny Porsche and Erik Dahlin at Binol AB for advising on the metal cutting fluids-related questions and for conducting the oil tests.

Last but not least, I would like to thank Chalmers University of Technology for organizing and providing all the necessary equipment, training and means for this project.

List of Abbreviations

BSE Backscattered Electron

BUE Build-Up Edge

CVD Chemical Vapor Deposition

EDS Energy Dispersive Spectroscopy

EP Extreme Pressure

ESEM Environmental Scanning Electron Microscope

FCS Free-Cutting Steel

HSS High-Speed Steel

HV Vickers Pyramid Number

LOM Light Optical Microscopy

MCF Metal Cutting Fluid

MQL Minimum Quantity Lubrication

MWF Metal Working Fluid

NMP Non-Measured Points

PCBN Polycrystalline Cubic Boron Nitride

PVD Physical Vapor Deposition

R_a Arithmetical Mean Roughness

R_t Maximum Height of the Roughness Profile

R_z Average Maximum Height

S_{10z} Ten-Point Height

S_a Arithmetic Mean Height

SE Secondary Electron

S_z Maximum Height

Table of Contents

List of Figures

List of Tables

Background

This master's thesis is being part of the FFI-Testbed project (VINNOVA Project No. 2016-02506). Chalmers University of Technology is in collaboration with Gnosjö Automatsvarvning AB, Swerea IVF AB (Now: RISE IVF AB) and Binol AB for a case study.

Gnosjö Automatsvarvning AB, a company which specializes in automatic turning of complex parts for automotive and other industries, was the host for the practical part of this case study. The machining tests were conducted on a Traub TNL 26 CNC lathe. A sequence of high precision cutting operations were performed on free-cutting steel (FCS) in order to manufacture a small component used in automotive industry. Drilling and turning operations were performed using coated carbide drill bits and inserts. Samples of the worn tools and the machined components were collected and analyzed at Chalmers. Metal cutting fluid samples were extracted during the test and analyzed at Binol AB.

Aim

The regular manufacturing of these components involves the use of mineral oil as metal cutting fluid. As the modern manufacturing strives to become more aware of their impact on the environment, many companies invest to find a sustainable alternative for the mineral oil-based fluids. Numerous studies show that the vegetable oil outperforms the mineral oil in many aspects due to its high biodegradability, low toxicity and equally good machining properties.

This thesis work aims at determining the wear of machining tools as well as the surface roughness of the machined components as a result of switching the metal cutting fluid from mineral oil to vegetable oil.

1. Introduction

Metal cutting fluids (MCFs) – also referred to as metal working fluids (MWFs) – are widely used in metalworking processes in order to lubricate, cool and remove chips from the workpiece, tools, and machine. Using MCFs can facilitate a better surface finishing and improve tool life. A correctly chosen MCF will, in addition to its basic functionality, provide (1) corrosion protection, (2) less health threat to the operator, (3) less negative impact on the environment, and (4) reduce the operating cost. Additionally, having a high flash point is an extremely important requirement for neat oils as during metal cutting processes friction and pressure results in high amounts of heat and thus increased risk of fire. There are several types of MCFs: water-based, gas-based and oil-based (neat oils) that can be used with or without additives. The additives are used to improve overall machining performance by inhibiting foaming, preventing bacteria and fungi contamination, creating an anti-wear effect by forming a liquid film on the surface of the machined component and alleviating the high pressures acting on the tool.

MCF can be referred to as cutting fluid, coolant or lubricant. While some materials require no lubrication during machining, others do rely on a simple water-based lubricant or rather a more complex oil-based fluid whose composition is determined for that specific application by testing.

1.1 Importance of Cooling

The nature of the coolant determines its cooling abilities. Neat and extreme pressure (EP) neat oils show a poor cooling effect compared to aqueous fluids. In general, soluble oil, and semi-synthetic/synthetic fluids can be used with free-cutting steels (FCSs) in turning operations. Drilling, in addition to the aforementioned ones, can use fatty or EP soluble oil fluids. Coolants are essential in the machining operations involving high-speed steel (HSS) tools, but also commonly used with carbide tools. Using a coolant is a priority in cases where small components are manufactured at a high rate using several different tools concurrently.

Sliding and shearing processes on the tool-workpiece interface and on the primary shear planes are the main heat sources. The cutting fluid serves more as a coolant than a lubricant in the chip formation process (Figure 1) because it does not have direct access to the tool-chip interface (Kurimoto, Barrow, & Davies, 1982). To efficiently eliminate heat, the coolants must be able to have access to the heat generating surfaces such as the flank face. The best way to achieve this is by letting the coolant reach the most stationary components of the system. This will allow enough time for the heat to be transferred from the heat source. A configuration, in which the coolant is allowed to flow through the tool, is very effective in transferring the heat but also largely contributes to chip breakability. Different machining setups have been developed experimentally by researchers to enhance the cooling action by directing the coolant to the end clearance face or to the flank face by installing the tool upside down. Both configurations improve the cooling effect by retaining the heat from spreading from the flank face or by cooling directly the flank face.

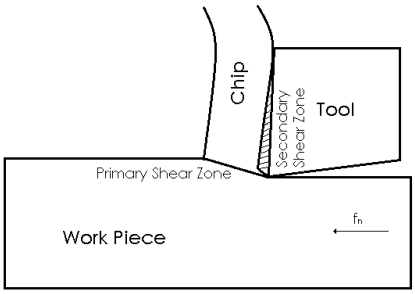

Figure 1: Tool-workpiece interaction

1.2 Substituting Mineral Oil

Mineral oils are used in machining extensively and make around 85% of the total consumption of MCFs worldwide leading to air pollution and contamination of soil and water (Shashidhara & Jayaram, 2010). Reports on EU MCFs consumption show that yearly, approximately 320k tones of oils are being used in the industry (Abdalla, Baines, Mcyntire, & Slade, 2006). Strict regulations on recyclability, environment pollution, health risks at work and many other factors have pushed companies and scientists to do research and come up with new solutions. Even though the global warming potential is much higher for mineral oil than that for vegetable oils, for many it is still the first choice due to its lower price.

The extensive research conducted on MCFs suggests that vegetable oil can be used as a substitute for mineral oil in machining without compromising the cooling, lubricating or chip removing ability. Table 1 presents the advantages that most vegetable oils have as well as a few disadvantages that can be fixed using proper additives (Shashidhara & Jayaram, 2010).

Triglycerides are the base structures that make up the vegetable oils. These glycerol molecules have three chain fatty acids that are believed to reduce wear and friction by means of their strong interaction with the metal surfaces (Siniawski, Saniei, Adhikari, & Doezema, 2007). Canola and rapeseed oils are among the most widely used base materials for biodegradable MCFs. Vegetable oils can show better scuffing load capacity, friction and wear properties than most mineral oils without additives (Lawal, Choudhury, & Nukman, 2012).

Advantages	**Disadvantages**
High biodegradability	Low thermal stability
Low pollution of the environment	Oxidative stability
Compatibility with additives	High freezing points
Low production cost	Poor corrosion protection
Wide production possibilities	
Low toxicity	
High flash point	
Low volatility	
High viscosity indices	

Table 1: Advantages and disadvantages of vegetable oil-based cutting fluids

1.3 Research on Vegetable Oil

Most vegetable oils do not meet the requirements for metal cutting in their raw state. In order to improve their characteristics, the oils must undergo some modifications such as sulfurization and phosphate modification. In a study by Jacob John et al. (2004), soybean oil was modified by sulfurization and ozonation to obtain a metal cutting emulsion. The interaction between the emulsion's components was analyzed and it was found that obtaining a stable emulsion out of this type of vegetable oil required a larger amount of surfactants to be added into the modified soybean oil than into regular soybean oil. Vegetable oil can provide better performance when its composition is reformulated by adding additives to promote a better load carrying capacity, improved tribological behavior and thermal stability, resulting in reduced wear and friction at the tool-chip and tool-workpiece interfaces. Similarly, the vegetable-based oils can be chemically modified by esterification and transesterification which are carboxyl group modifications and selective hydrogenation, metathesis, oxidation, the formation of C-C and C-O bonds, dimerization and oligomerization which are fatty acid chain modifications (Shashidhara & Jayaram, 2010). The vegetable oil-based MCFs made from genetically modified seed crops require less modification and have proven to have a better thermal and oxidative stability as well as a higher load carrying capacity (Shashidhara & Jayaram, 2010). It was found that machining stainless steel was better done when using vegetable oils with natural additives and resulted in lower cutting forces as well as lower friction values when compared to commercial mineral oil (Shashidhara & Jayaram, 2010). The latter had more advantages in machining aerospace-grade titanium alloys.

The performance of commercial vegetable oil-based cutting fluid as well as formulated blends of rapeseed and other oils have been tested in drilling operation to assess several parameters such as tool wear, tool life, and cutting forces. The reference mineral oil showed poor performance compared to the formulated blend consisting of rapeseed and ester general purpose oils leading to a 177% difference in tool life. The chip tangling percentage was registered as the lowest with the same formulated oil. In terms of flank wear, all the vegetable oil blends outperformed the mineral oil by twice as much (Belluco & Chiffre, 2004).

In a study review by Lawal et al. (2012), it was found that machining AISI 304 austenitic stainless steel using coconut oil resulted in better surface finish as well as reduced tool wear when compared to machining with mineral oil. Coconut oil was also found to diminish cutting temperatures and reduce surface roughness and tool wear better than SAE-40 mineral oil when machining AISI 1040 steel. Minimum quantity lubrication (MQL) with palm oil in machining AISI 420 steel led to more gradual tool wear compared to dry and flood lubrication types. Overall, there has been plenty of research conducted on ferrous materials and not so much on non-ferrous materials such as aluminum, copper and brass as well as superalloys such as nickel-, cobalt- and iron-base materials. Vegetable oil-based MCF has proved to be a good alternative to the mineral oil-based. Even though some sources claim there is significant tool life improvement as well as reduction in thrust when using the former, the resulting outcome is always dependent on the type of material being machined (Lawal, Choudhury, & Nukman, 2012).

In research by De Chiffre et al. (2002), several machining operations were performed on austenitic stainless steel using mineral, synthetic and vegetable oil-based fluids to evaluate cutting forces and tool life in different setups. It was found that both the

parameters improved in the case of machining with vegetable oils and esters. The use of vegetable oil emulsion resulted in the best tool life in both drilling and turning operations with over 300% and 140% performance index respectively, followed by synthetic based esters with over 180% in drilling and over 125% in turning operations (reference 100% for the mineral oil emulsion). In the case of straight oils, drilling tool life was the highest when using vegetable/ester mixture with less than 10% EP additives, followed by ester oil and by vegetable/ester mixture with less than 5% EP. Stamping operation tests were performed with soybean, olive, corn, and sunflower oils. The best performance was registered in the case of olive oil. All vegetable oils performed better than the mineral oil in terms of surface topography, but were not able to provide as good boundary lubrication as the mineral oil. In deep drawing operation tests, the use of canola oil combined with boric acid resulted in a decrease of 44% in friction. It was concluded that this type of mixture is able to improve formability and surface roughness of the steel sheet in deep drawing operations.

Groundnut oil has also been used as an MCF in the machining of stainless steel. It has shown better results compared to a 20% mineral oil emulsion. Due to its superior lubricating properties, the use of vegetable oil led to a 58.3% decrease in surface roughness. As a coolant, it did not perform as well as the emulsion being 7% less efficient in removing the heat from the cutting zone (Ogedengbe, Awe, & Joseph, 2019). Groundnut oil has also been compared to palm oil and to conventional mineral oil to assess its performance in mild steel machining under different cutting parameters. It has a high viscosity index and results in good surface roughness, therefore the author suggests that it can replace the conventional cutting fluid. Lemon fruit extract has been used with this oil to improve its oxidation properties (Kolawole & Odusote, 2013).

In a study by Bhowmik et al. (2015), the performance of coconut and sunflower oils has been compared with the conventional mineral oil. The neat oils have been applied by MQL method in turning of aluminum AA1050. This lubrication method requires direct application to the contact zone between the tool and the workpiece. The results showed that the surface roughness, Ra, of the machined components was better when machining with coconut oil at higher cutting speeds and medium feed rates, most of the results indicating that this cutting fluid performs better or as well as the reference mineral oil.

1.4 Surface Roughness Evaluation of the Machined Components

The surface roughness of the machined component does not only influence the appearance of the final product, but can as well be of immense importance in its functionality such as lubrication ability, wear resistance, friction coefficient and corrosion resistance.

The surface roughness values of a machined component can either be calculated on a profile or a surface. Thus, two different sets of parameters, such as R_a, R_y, and R_z for a line-scan as well as S_a and S_q for an area-scan, can be obtained. Even though area roughness parameters are more meaningful and better characterize a surface, the profile parameters are more commonly used to describe surface roughness on a technical drawing. The average roughness, R_a, is measured in micrometers and varies between different manufacturing processes from 0.01 µm in superfinishing to 25 µm in shaping and planning. In turning and drilling operations, R_a values range from 0.19 µm to 6.3 µm and 1.6 µm to 6.3 µm respectively (“*Exploring surface texture*”, 2011).

After machining, surfaces tend to have irregularities which, depending on their height and spacing, make a surface smooth, rough, curved or wavy. It is common to have a combination of roughness and waviness, sometimes accompanied by form error. There are several techniques for reading a surface. One of the simplest and most common contact techniques to record surface irregularities uses a sharp stylus to register changes in amplitude. The stylus travels over a certain area at a constant speed. Then, the obtained electrical signals are amplified and displayed in a readable for the operator way. As the stylus is in contact with the surface, its ability to detect small features is limited to the tip diameter. The patterns left on the surface by the tools are referred to as lays. Measured traces can be taken perpendicular or at an angle to the lay depending on the lay type. It is common practice to take perpendicular to the lay direction trace measurement as this way the trace will include the maximum number of points. The digital representation of a surface might be influenced by several factors including the stylus tip geometry, mechanics and electronics, digitization, calibration of the system, arcuate correction, form removal, and specific filters applied.

Another commonly used surface roughness measurement technique is the optical interferometry. This is a non-contact measurement technique that has several advantages over the contact techniques including the possibility to measure surfaces that are difficult to access physically, a larger measurement range and a higher precision and resolution (Wang, Xie, Ma, & Dong, 2017). It uses light to accurately determine the height variations. A beam of light passes through a beam splitter forming a reference and a measurement beam. Optical interference occurs for every point on the sample's surface where the lengths of these two beams, between the reference mirror and the beam splitter and between the sample surface and the beam splitter, are the same. A designated software is used to compute the topography from the interference patterns captured by means of a video camera.

It is important to note that a graphical presentation of a measured profile is a magnified representation of the actual surface texture but with different horizontal and vertical scales. It clearly describes the peaks and valleys in the profile but misrepresents the irregularity spacing as in reality, the height of the irregularities is much smaller than their spacing.

Artificial neural network models have been used to understand the correlation between the surface roughness and the cutting parameters used in the turning process of FCS. R_a and R_t parameters show high dependency on the cutting speed and on the feed rate. It was demonstrated that increasing the cutting speed and decreasing the feed rate lead to lower surface roughness (Davim, Gaitonde, & Karnik, 2008). Similar results have been reported by Debnath et al. (2016) in their study of turning mild steel with coated carbide inserts. They found the feed rate to contribute the most, decreasing the surface roughness by 34%. Low-flow high-velocity application of cutting fluid showed a similar effect on the surface roughness, a reduction of approximately 33%.

1.5 Research on Tool Wear Mechanisms

The wear mechanisms of a machining tool depend on the cutting parameters, tribological and chemical properties of the interacting surfaces, lubricity, temperatures surrounding the cutting zone, cutting forces, the presence and type of coating on the tool as well as the amount and type of coolant. Consequently, a worn tool can be characterized by diffusion, adhesive, oxidation, fatigue and abrasive wear mechanisms. Various coatings

are used in order to improve the wear characteristics of a tool. A coating can serve as a protective barrier that impedes diffusion between the tool and the workpiece, improves the surface hardness and wear resistance of the tool, decreases the friction coefficient and thus the abrasive wear, minimizes adhesion and keeps the tool substrate temperature down. All these have a significant impact on the tool life, surface finish and the final properties of the manufactured components.

The removed material can pile up and reduce accessibility to the clearance face raising the cutting temperatures. It was found by Kurimoto et al. (1982) that the crater wear is closely related to the fluid's cooling ability. High cutting temperatures often lead to diffusion and often result in crater wear with the maximum crater depth point being at the maximum temperature location.

In research by Xu et al. (2012) on tool wear in FCSs, it was found that crater wear on the uncoated inserts is much more pronounced than on the coated tools with multilayer coating. The reason for that is the poor heat dissipation of the coating compared to the substrate that leads to the majority of heat being removed by the chip when turning with a coated tool. Thus, the uncoated tool was found to have more significant wear on the rake and flank faces and in addition to all the wear types present in the coated tools it has also gone through oxidation wear. Unlike the uncoated tools, the coated inserts showed to benefit more from the manganese sulfide (MnS) inclusions which formed a lubricant zone along the cutting edge. This not only improves machinability but also minimizes the tool wear by inhibiting diffusion and decreasing the cutting forces. Lower cutting forces lead to lower power consumption. The author also claims that the micro-voids generated by the inclusions in the ternary shear zone can reduce the flank wear.

Gu et al. (1999) studied the effect of coatings on the flank wear and the wear mechanisms of coated and uncoated milling inserts. Tool life was found to be dependent mostly on the cutting speed and less on the feed rate and was longest for the TiAlN coated inserts, followed by TiN and ZrN coated tools. The tool wear was influenced by build-up edge (BUE) formation at low cutting speeds and by high temperatures when the cutting speed increased. The uncoated tools were reported to wear by micro-attrition, micro-abrasion, fatigue, thermal fatigue and chipping while the coated ones were worn by abrasive wear (on coatings) and micro-attrition, attrition, and abrasion. It has been found that a 2.8 μm thickness is optimal for a physical vapor deposition (PVD) TiN coating on HSS tools when machining FCSs. Similar results were reported by Junior et al. (2008) on milling inserts after machining stainless steel. In this study though, vegetable oil-based cutting fluids were used instead of the conventional mineral oil-based fluids. Among the tested fluids and application methods were vegetable oil-based emulsion flood, neat vegetable oil applied by MQL method and neat vegetable oil at low flow. For specific machining parameters, the neat vegetable oil at low flow led to the longest tool life, almost double than when machining dry or with emulsion. All the cutting methods under investigation showed wear by abrasion and adhesion. It was also reported that adhesion on the coated surfaces was not observed. Vegetable oil application by MQL has also been done in turning AISI-1060 and AISI-9310 steels and resulted in improved tool life for the uncoated carbide inserts and better surface finish compared to dry machining (Khan & Dhar, 2006; Khan, Mithu, & Dhar, 2009). In a different study by An et al. (2014), the effectiveness of MQL has been tested in thread turning of AISI-1215 FCS and it was found that the cutting forces were 60% lower than in dry machining.

Tamerabet et al. (2018) investigated the tool wear in dry machining of carbon steel (SAE 1030). The material was turned with different carbide inserts coated by chemical vapor deposition (CVD): KC810 (TiN+Ti(C,N)+TiN coating) and KC910 (TiC+Al_2O_3 coating). Dry machining caused elevated temperatures and led to excessive tool wear that included thermal flaking, BUE, deformation, and fracture of the cutting edge. The authors suggest using PCBN tools for precise and dimensionally accurate machining and using CVD coated carbides whenever tool life is a priority. For a certain set of cutting parameters, it was found that for KC810 insert the tool life was much longer than that of KC910 insert (288 min and 35 min respectively).

A study by Hoier et al. (2019) describes the tool wear of coated and uncoated carbide tools in turning operation of tool steel and stainless steel. It reveals that the main wear mechanism when machining tool steel is abrasion wear. Machining stainless steel with coated tools resulted in micro-fragmentation and localized chipping while the use of uncoated tools led to dissolution wear. The flank wear developed much faster for the uncoated inserts than for the coated inserts for both tool and stainless steels. The cutting forces decreased substantially when machining tool steel with coated inserts and not as much when machining stainless steel.

High temperatures generated at the tool-chip contact zone trigger the start of dissolution wear. This type of wear was found to be the predominant wear mechanism on the crater face in machining lead-free and leaded FCSs with carbide tools. Methods to suppress the dissolution wear such as the introduction of engineered deformable oxide inclusions and HfN coating have been proposed by Ramanujachar et al. (1996). The tool wear by dissolution and abrasive wear is not as pronounced when machining Ca-S FCSs. The reason for this is the formation of an adhering layer on flank and rake faces of the insert. This shielding layer of compound ternary oxides improves significantly the tool life and leads to better machinability when compared to regular stainless steel. A similar layer of aluminum and nitrogen was found on carbide tools after machining BN FCS at high cutting speeds. It is believed that this layer has influenced the overall tool wear and led to reduced cutting forces. The flank and crater wear in machining BN FCS are twice lower than when machining regular steel (Fang & Zhang, 1996).

1.6 The Role of Inclusions in Machining

Machinability can be described by tool wear and the resulting surface quality of the machined component, depending on certain parameters that closely interact with each other. These include the work piece material, the cutting tools, the cutting fluid, and the machining parameters. The workpiece material depends on the composition, microstructure and non-metallic inclusions. Extensive research on FCSs suggests that its machinability largely depends on the non-metallic inclusions and discusses how the inclusions' size, number, distribution, composition, and morphology affect the metal cutting process. It is known that in FCSs the unit power consumption increases with decreasing the sulfur (S) content and with increasing the material hardness. A study comparing free-cutting stainless steel to regular grade revealed that increasing the S content to 0.1% leads to a 50% reduction in flank wear and 25% reduction in cutting force in a turning operation. Addition of MnS of up to 1% by volume can significantly improve machinability, above that only minor improvement can be achieved (Ånmark, Karasev, & Jönsson, 2015). Even though there are numerous advantages of having MnS inclusions in the steel, the disadvantages such as decreased cold brittleness, high

corrosion, anisotropy in mechanical properties, poor weldability and toughness should not be left aside (Ånmark, Karasev, & Jönsson, 2015).

Lead (Pb) is a strictly regulated element and is regarded as harmful. This does not stop it from being widely used in the production of FCSs in order to improve the tool life and the surface quality (machinability) of the machined components. The use of Pb adds lubricity to the material and makes the FCSs more fragile (brittle) during machining.

A study by Zhang et al. (2009) defines the effect of sulfide inclusions' shape and size on machinability of FCS. They compared between spindled (elliptical) and stripped shape sulfides. In the case of TiN coated carbide inserts, it was found that surface roughness of the machined components is better in materials with small sulfide inclusions. Having smaller inclusions can also contain the formation of some defects such as burr and cave (Zhang, An, Zhang, Liu, & Chen, 2009). A bigger sulfide size can facilitate the BUE formation thus modifying the tool geometry and consequently worsen the surface quality. The tool wear is not influenced by the size and shape of the sulfides when using coated tools. The reason for that is the high cutting speed used with coated tools which does not allow enough time for the material to fully plastically deform thus hindering the increase in deformation stresses. High cutting speeds result in higher temperatures that melt the MnS inclusions making them too soft to form a protective layer. The chip formation in machining FCS does not change with sulfide size or shape in the case of coated inserts. When it comes to the uncoated carbide inserts though, both the flank wear and the chip breakability and thus the chip shape change with different sulfides. The spindled sulfides would both facilitate lower flank wear and the formation of short C shaped chips as opposed to a larger flank wear and long curly chips in FCSs with striped sulfides. The spindled sulfides act as stress concentrators and whenever a force is applied, an agglomeration of micro-cracks formed will coalesce to form the chip rupture.

The size and the distribution of MnS inclusions have an influence on the BUE formation. Uneven distribution of coarse MnS can cause the chip to break far away from the tool's cutting edge. The material between the tool and the chip breaking point will remain on the tool as BUE. Uniformly distributed sulfide inclusions on the other hand cause less stress concentration and the chip breaks closer to the tool, leaving less material on the tool. In their study, M. Hashimura et al. (2009) found that machining a coarse MnS FCS will result in a larger BUE formation when compared to fine MnS FCS. Similarly, the latter will lead to better surface roughness as well as less flank wear and lower cutting forces. It was observed that a larger BUE would result in a rougher surface of the machined component.

MnS is known not only for its ability to reduce the friction coefficient, but also to decrease the flow stresses in the primary and secondary shear zones. In a study by Yaguchi (1986), it was found that the BUE formation starts at higher cutting speeds when increasing the size of the sulfide inclusions or its amount in the material. The study also shows how the BUE size grows with decreasing the sulfide size (observed in high-speed steel tools). It was observed that BUE size tends to be lower in places where MnS deposits, acting as a diffusion barrier, are found. Very small sulfide inclusions are known to be ineffective in serving as deformation barriers, acting as crack initiation sites. They are either too small or too soft to resist deformation and thus are carried along within the material being removed, causing the BUE to grow further. It is discussed among the researchers that due to the slightly higher hardness of sulfides (impure sulfides) compared to the matrix, they deform less and tend to produce micro-voids, when the

material is deformed, and thus reduce the shear strength. The temperature at the contact point between the tool's BUE and the workpiece can thus be related to the size and type of MnS inclusions. Since heat is generated during the plastic deformation of the material and depends on the shear strength, the presence of sulfides can impede the temperature rise by lowering the effective shear strength and the frictional force at the tool-chip interface.

It has been found that the cutting force and flank wear in the machining of FCSs are reduced by MnS inclusions better than by other sulfides. In his study, Laizhu et al. (1996) found that the cutting force is dependent on the shape of the inclusions and is lower with elongated sulfide inclusions than with globular ones. The globular inclusions, on the other hand, were more effective in decreasing the flank wear. A higher percentage area of the sulfide inclusions was found to be beneficial for both the flank wear and the cutting force. It has been found that surface roughness decreases when the FCS is Ca treated. The author studied the elongation behavior of the inclusions and their shear deformation in the primary shear zone observing that the inclusions change their orientation in the cutting process. They claim that the shear angle varies with the sulfide type and is highest for MnS inclusions, followed by (Mn, Ca)S. In a similar way, the authors describe the effectiveness of the sulfides in the crack generation and relate the deformability of inclusions to the cutting forces, saying that the MnS inclusions in the re-sulfurized FCSs have the highest deformability and result in the lowest cutting forces. As described by different researchers, this study agrees that the cutting force increases as the space between the inclusions increases, and decreases when the inclusions' area percentage increases. It is suggested that the MnS inclusions are not as effective in the third shear zone as the other types of sulfide inclusions because the compressive stresses there are higher and tend to close easier the voids created by the softer inclusions (the ones which are more deformable). BUE size was similarly found to be dependent on the deformability of inclusions and is partially affecting the surface roughness of the workpiece. Sulfide inclusions have been found to cause the BUE to fall off, this can either improve or worsen the surface roughness of the workpiece depending on how much BUE is being adhered and how much of it is being smeared on to the surface (both partially dependent on the inclusion size and percentage area).

A study by Hazra et al. (1974) describes the behavior of MnS inclusions in the machining of FCSs. With the help of a scanning electron microscope (SEM), it was observed that during deformation in the shear zone the sulfide undergoes decohesion from the matrix, cavitation and cleavage fracture (at 90˚ to the compression direction), and thus agreeing with the other findings that describe the micro-void formation at the inclusion site. The test was performed at low cutting speeds such as to maintain the cutting temperature as close as possible to room temperature, possibly resulting in the brittle behavior of the inclusions. Otherwise, in high speed cutting, the MnS inclusions would melt improving the lubricity in the machining process.

It was found in a series of uniaxial compression tests, SEM and high-resolution transmission electron microscopy (HRTEM) analyses (Qin, Xia, Ma & Zheng, 2017) that inclusions act as deformation inhibitors for the crystalline grains thus, improving the fracture strength in FCSs. Wang et al. (2015) investigated the effect of BN and MnS inclusions on the machinability of FCSs by nano-indentation measurements. The hardness of these inclusions is lower than that of the matrices and the difference in the elasticity between the matrix and the inclusions causes crack nucleation. The author

claims that soft inclusions like MnS can prolong the tool life by enclosing harder particles such as Al_2O_3 and TiN.

2. Experimental Procedure

The works conducted in this master's thesis as well as how the obtained results were achieved are described in this section, covering the machining test, metallographic sample preparation, microstructural characterization and inclusions analysis, hardness test, roughness evaluation of the machined FCS surfaces, tool wear analysis and oil analysis.

2.1 Machining Test

Traub TNL 26 CNC lathe with an isolated coolant tank was used. The test was run for four weeks and involved the same machining operations while changing the cutting fluid every week. Machining with 100% mineral oil, considered to be the reference point for this test, in the first week, was followed by machining with 100% vegetable oil in the second week, a mixture of 50% mineral and 50% vegetable oils in the third week, and a mixture of 75% mineral and 25% vegetable oils in the fourth week (See Table 2).

Week 1	**100% Mineral Oil**
Week 2	100% Vegetable Oil
Week 3	50% Vegetable Oil + 50% Mineral Oil
Week 4	25% Vegetable Oil + 75% Mineral Oil

Table 2: Test plan

Drill bits used in one of the drilling operations were collected at the end of each week (before the end of their tool life) and carbide inserts used in the turning operation were collected at the end of their tool life for tool wear analyses. The tool wear mechanisms were studied at Chalmers using environmental scanning electron microscope (ESEM) and light optical microscopy (LOM). A piece of FCS sample from the raw material was obtained from Gnosjö for microstructural characterization and hardness tests.

Oil samples were collected at the beginning of every week, soon after the machining started, and at the end of each week after the production has been stopped. Oil samples were then sent to Binol AB for purity and viscosity tests.

In order to determine how the cutting fluids interact with the tools and the tool-workpiece interface, the first and the last machined component for each of the inserts were collected throughout the test. At RISE IVF, a 3D optical profiler was used to conduct the surface roughness/morphology evaluation on all the machined components.

To minimize the complexity of the case study, constant cutting parameters, constant number of machined components per tool, same batch raw material and same batch cutting tools were used throughout the entire test.

2.2 Sample Preparation for Metallography

Samples have been prepared such that the microstructure in the rolling direction of the material is revealed. A cross-sectional disc from the FCS bar has been cut into a cuboid using a Struers Discotom 2 abrasive cutting machine in order to evaluate the

microstructure on two of its sides, at a 90˚ angle, to see if there is any difference in the inclusions. Subsequently, the cuboid was cut into triangular shapes (see Figure 2). A second cross-sectional disc was cut to perform hardness tests on. The discs were sectioned by horizontally positioning and tightening the steel bar in the cutting chamber. The sectioning was done wet (water cooling) to prevent any changes in the microstructure using an Al_2O_3 abrasive disc and a light pressure exerted by hand to the cutting handle. Sampling was done away from the ends of the FCS bar.

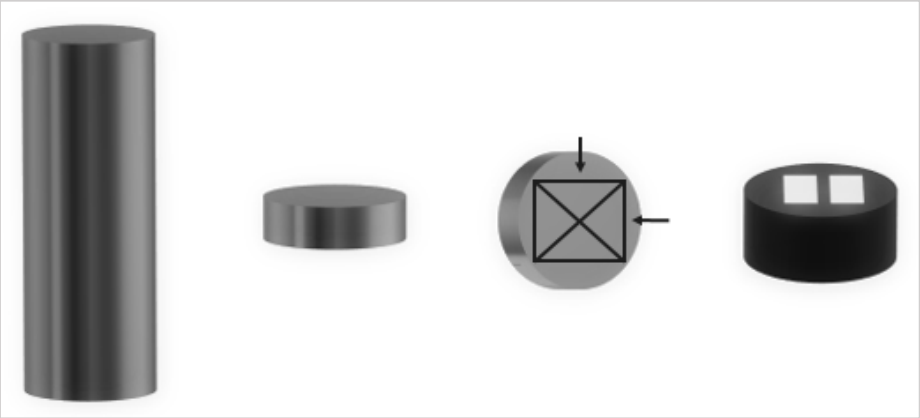

Figure 2: Sample sectioning

After manually grinding the burrs formed during sectioning, the samples were mounted into 40 mm molds of PolyFast conductive resin (suitable for SEM), such that the two side faces of the rectangular parts are in the same mold and the circular sample is in a separate mold. The samples were mounted on a Struers Citopress-20 mounting press at a temperature of 180° C and a pressure of 250 bars.

The grinding and polishing operations were performed on a Struers Tegraforce-5 automated polishing machine that can operate with up to six samples at a time. To grind the samples, grinding papers of #120, #320 and #800 grit sizes were used, the larger grit size resulting in a finer surface finish. Polishing the samples required the use of polishing discs and diamond polishing suspensions and was done in three steps using 9 µm MD-Largo fine grinding composite disc, 3 µm DP-Dac and 1 µm Nap polishing discs. After each grinding step, the samples were properly washed to avoid any large particles left on the sample that could scratch the surface in the subsequent grinding steps where a finer grit was used. During polishing water contact was avoided in order to eliminate sample oxidation, instead, the samples were flushed with isopropanol. After the final polishing step, the samples were cleaned with ethanol and dried in a stream of mild air. It is important to not let the alcohol dry on the surface but blow it away instead. Sometimes, it can also be necessary to clean the surface using some soft cotton wool in order to obtain a mirror-like surface suitable for microscopic analysis. The sample prepared for metallography has been etched to reveal the microstructure using a 1.5% nital reagent.

2.3 Raw Material Analysis

FCS bars of 25 mm in diameter have been used in machining small, complex and high precision components for the automotive industry. The high production volume of these components involves a series of cutting operations performed on the raw material. This study investigates only two of them: turning and drilling. Throughout the test, steel bars from the same batch have been used in order to eliminate any variations in the microstructure, hardness and mechanical properties of the material. The chemical composition for the material investigated is represented in Table 3.

	C	Si	Mn	P	S	Cr	Ni	Mo	Pb	Al	Cu	N
wt%	<= 0.12	<= 0.03	0.90 1.30	<= 0.100	0.290 0.330				0.20 0.35			
	0.07	0.02	1.24	0.047	0.320	0.11	0.09	0.02	0.22	0.002	0.19	0.009

Table 3: Chemical composition in wt%

2.3.1 Microstructural Analysis

ESEM and LOM have been used in order to evaluate the microstructure. Different ways to determine the pearlite area percentage in the microstructure have been considered. One way to do so is by using the ImageJ software to calculate the percentage of pearlite from the ESEM images. The threshold adjustment was done individually for each image in order to achieve the best selection possible. A total of 36 images (equivalent to 8.67 mm²), taken using a Philips XL-30 ESEM with a secondary electron detector (SE) at 12 kV and 500x magnification, were analyzed by ImageJ.

Several images at different magnifications, 10x, 20x and 50x, have been taken at different spots on the sample surface using a Leica LEITZ DMRX LOM equipped with a Zeiss AxioCam MRc 5 camera. Knowing the area percentage of the inclusions, it is possible to analyze LOM images (Figure 6, b) with ImageJ software by adjusting the threshold such that to select both inclusions and the pearlite phase together (see Figure 19). Knowing the area of these constituents makes it easy to find the pearlite area by subtracting the already known area of inclusions from the result. The total analyzed area of LOM images is 10.15 mm² (equivalent to 7 LOM images at 10x magnification).

A third method to determine the area of pearlite comprises the analysis of the same 10.15 mm² area from LOM images using a programming software called Python. A code that replaces the pixels which are close in color to pearlite with white pixels has been written. The combination of different amounts of red, blue and green colors allowed to determine the color range for the brown appearance that the pearlite has on the images. The program counts the number of replaced pixels and calculates the area percentage of them outputting the result value (find the code and the pixel replacement process in the Appendix).

2.3.2 Inclusions Mapping

Machinability of steels is significantly improved by adding different chemical elements such as Pb and S to their composition. Both these elements can form low shear strength

inclusions that have a lubricating effect on the cutting process and improve the chip breakability as in the case of MnS inclusions which act as stress concentrators.

Microscopic test methods have been used according to ASTM standards for determining the inclusions content in steels. Two 15 x 8 mm samples, that were mounted in the same mold, have been analyzed using ESEM. According to the standard, ASTM E45-18a, an area of 160 mm² polished sample surface is sufficient for the analysis. In this study, a total area of 240 mm² has been used to make a series of images distributed evenly over the entire sample following a specific scanning pattern (Figure 3) to avoid the analysis of local variations and obtain a result that would characterize the entire sample. A total of 26 images (equivalent to 6.8 mm²) were taken on each sample at 12 kV and 500x magnification by means of Philips XL-30 ESEM and a backscattered electron detector (BSE).

An Oxford INCA energy dispersive spectroscopy (EDS) system, integrated into the ESEM, has been used in order to determine the nature of the inclusions. This technique gives the elemental analysis of the sample. Atom excitation results in an isotropic emission of X-rays, some being trapped inside the material. The X-rays having a higher energy are more likely to escape the sample and reach the detector. A number of point analyses have been performed on random inclusions to compare the obtained spectra.

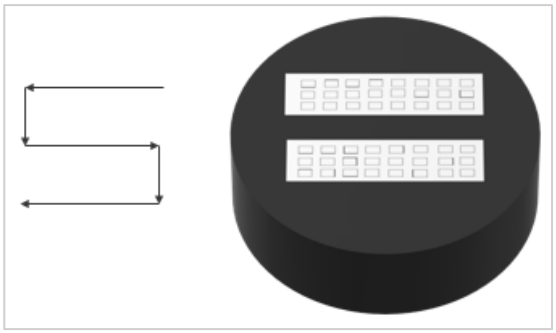

Figure 3: Sample scanning pattern

2.3.3 Inclusions Calculation

In order to determine the size and the area percentage of the inclusions, a software called ImageJ was used. The taken images were uploaded to the software and the scale was converted from pixels to micrometers. Threshold adjustment allowed to automatically select and count the MnS and Pb inclusions separately. Eliminating the noise resulted in more precise thresholding and area/volume calculation.

2.3.4 Hardness Test

In a hardness test, an indenter of a specific shape, usually made from a harder material than the tested specimen, is forced into the sample. The ability to withstand the deformation induced by the indenter is called hardness.

The Vickers hardness test was performed on a 25 mm diameter cross-section sample in accordance with the ASTM standard test method for micro-indentation hardness of materials. This test method uses a diamond pyramid with a 136˚ interfacial

angle. The steel sample was impregnated in resin, ground and polished to ensure that its surface will be normal to the indenter's application direction. Application of a higher load leads to the generation of pileups around the indentation site due to plastic deformation. With this in mind, the load must be selected such that the indentation diagonals be larger than the microstructure constituents in order to avoid having localized results. A load of 0.2 kgf was applied for 10 seconds. The distance between the indentations as well as between the center of the indentation and the edges of the specimen was longer than 2.5 times the diameter of the indentation.

Measurements have been taken in two parallel lines from the periphery towards the center of the specimen as represented in Figure 4. The test assumes no elastic recovery after the indenter is retracted.

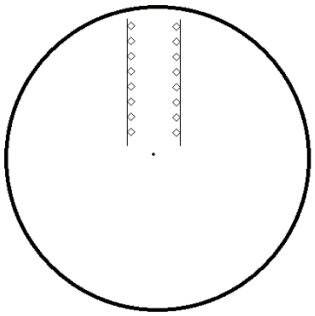

Figure 4: Indentation pattern

A total of 20 indentations have been made using the Struers DuraScan hardness tester. The results are plotted in Figure 9 in the Results and Discussions section, blue data points representing the measurements along the line on the left side of the sample. The Vickers hardness has been calculated automatically by the software through automated image analysis but can also be found manually by the formula:

$$HV = 0.9272\frac{\mathrm{P}}{\mathrm{A}} + \frac{2Psin(136^{\circ}/2)}{d^2} \approx 1.8544\frac{P}{d^2}$$

where P is the applied load in kgf, A is the indentation area and d is the arithmetic mean for the measured diagonals d1 and d2 (See Table 6 in Appendix).

2.4 Roughness Evaluation of Machined Surfaces

One of the benefits of the FCSs is the possibility to obtain a good surface finish at relatively high cutting speeds. Using a properly selected cutting fluid can help improve the surface quality by reducing the BUE formation. The addition of Pb is also known to have a positive effect on the surface roughness. In this test, the machining of a series of small and high precision components for the automotive industry has been performed using four mineral and vegetable oil-based cutting fluids. It was necessary to determine if changing the conventional mineral oil to commercially available vegetable oil or to a mixture of both would cause any changes in the surface roughness. It should be noted

that old mineral oil has been used in a mixture with new vegetable oil. It is unknown however how much time the old mineral oil has been kept in use.

S Neox 3D optical profiler with Nikon DI 10X objective has been used to conduct surface roughness measurements on cylindrical components turned with TiCN-coated carbide inserts. A total of 35 samples were analyzed after being cleaned from residual oil for ten minutes in an ultrasonic bath, fully immersed in acetone, then flushed with isopropanol and thoroughly dried with a stream of air. Several measurements on the same component resulted in similar results. It was decided that for the turned cylindrical parts one areal measurement per component is sufficient. The three-dimensional surface was scanned to create a topography layer filled with data points. The non-measured points (NMP) ratio was kept below 1% and filled in automatically by the software.

When flattened, the measured area consisted of 1360 by 1024 points with a 1.29 µm spacing. A set of surface parameters was registered, these being arithmetic mean height (S_a), Maximum height (S_z), and ten-point height (S_{10z}). By extracting profiles from the areal scan, it was possible to calculate the arithmetical mean roughness value (R_a), average maximum height (R_z), and maximum height of the roughness profile (R_t). Each of these values has been recorded as average over ten extracted profiles (see Figure 5, b).

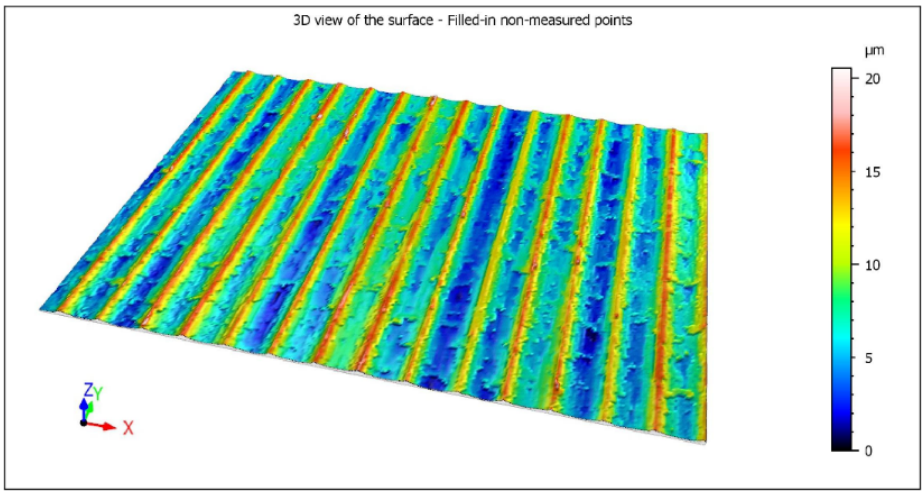

a) 3D surface

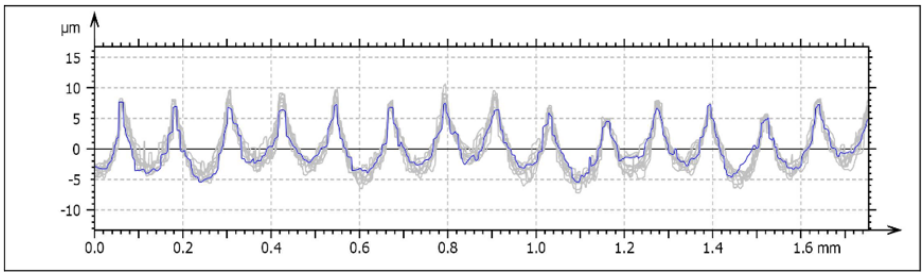

b) 2D profiles

Figure 5: 2D profiles extracted from a 3D surface (in the feed direction)

2.5 Tool Wear Analysis

Turning and drilling operations have been performed on FCS using mineral and vegetable oil-based cutting fluids. The primary goal of this study was to determine any correlation between the cutting fluid and the tool wear. Carbide inserts and drill bits have been analyzed using ESEM/EDS techniques. Same batch tools have been provided for this test so that any tool related variations are excluded. The examined inserts have come to the end of their tool life while the drill bits, having a longer than the test period tool life, have been collected at the end of each week (refer to Table 2) during the machining test. Only one drill bit has been used with each cutting fluid and thus the wear on the drill bits cannot be considered when assessing the performance of the tested cutting fluids as the sample number is too low. The number of machined components per tool has been kept constant (as close as possible) to avoid any variations in the tool wear due to the machining time.

The same ESEM/EDS equipment mentioned before has been used to analyze drill bits and cutting inserts. Images of the drill bits have been taken from the top view using the BSE detector, at 12 kV and 55x, 100x and 650x magnifications. The larger magnification images were used for measuring the flank wear on every cutting edge. Every insert has two cutting edges. Each of the cutting edges was imaged using ESEM's both detectors, SE and BSE, at 150x and 200x magnification on the top view (rake face) and 250x and 350x magnification on the side view (flank face). Larger magnification images of up to 3500x have also been taken for a more detailed observation of both the tool types. Elemental mapping and point analyses with EDS have been done on all the cutting edges for both drill bits and cutting inserts in order to determine the type of substrates and coatings.

2.6 Oil Analysis

The composition of the oils used in this study will not be disclosed. The properties of metal cutting oils are significantly enhanced by the additives in their formulation. These can be fungicides, bactericides, antiwear (AW) additives, EP additives, corrosion inhibitors, foam inhibitors, antioxidants, wetting agents, etc. Addition of chlorine and sulfur as EP additives helps to avoid chip welding by creating a protective coating on the tool surface. Once in contact with metal surfaces, additives can form metal salts that reduce cutting forces and heat generation. With all the benefits, increasing the volume percentage of additives in a cutting fluid decreases its biodegradability.

The machining process has been conducted for four weeks, changing the cutting fluid at the end of each week. Oil samples have been collected at the beginning and at the end of the weeks in order to determine their purity and viscosity. In order to have a uniform mixture of the two oils, the first samples have been collected after running the CNC for several hours. A visual examination of the samples showed no layering in the mixtures. In the purity test, 0.8 μm filter paper has been used to filter 100 ml of oil. The particles caught on the filter paper were counted using an optical microscope. In the viscosity test, oil at 40º C has been evaluated using an Ubbelohde viscometer.

2.7 Limitations

It is common to have variations in the raw material even within the same batch. Variations in the mechanical properties of the material might have a different impact on the tool wear. These variations remain unknown as testing of each metal billet separately is not cost- and time-effective.

Machining with several different cutting fluids while keeping constant the machining parameters might not be efficient. Differences in lubrication, cooling and chip removal ability between the mineral and vegetable oils might require a change in some machining parameters in order to optimize the cutting process. It was assumed that these differences do not impose any changes in the cutting forces or the temperatures at the cutting zone.

When preparing the oil mixtures, it was difficult to measure the exact amount of oil. The use of a metering pump would have solved this issue. Difficulty to completely drain the machining fluid from the CNC, prior to filling up with a new one, might have slightly influenced the intended percentage of each oil in the mixture.

We can only assume that the initial tool geometries were the same.

Owing to the limited time and resources, a prolonged machining test and repeatability test could not be done within the project period. Still, a study by Chiffre et al. (2000) gives us some hints about the repeatability in a machining test. It discusses the repeatability and resolution of a series of tests performed on turned and drilled components using different material types and several cutting fluids. It reveals that repeatability and resolution are the best for cutting forces tests, followed by tool life tests and by surface roughness tests with the lowest repeatability of all.

3. Results and Discussion

3.1 Raw Material

3.1.1 Microstructural Characterization

Machinability of FCSs is highly dependent on their composition. As it was discussed before, the addition of S and Pb can significantly ease the cutting process. Addition of a high amount of Mn ensures that all the sulfur will be formed into MnS inclusions. Elongated pearlite regions evenly distributed in a softer ferrite phase represent the major constituents in this microstructure (see Figure 6). The pearlite phase consists of ferrite and cementite lamellae.

It is known that, in this particular steel, the tool life of the coated carbide inserts and drill bits is very dependent on the amount and distribution of pearlite which changes from batch to batch. Since pearlite is the hardest phase in this material, a higher pearlite volume leads to a shorter tool life. Ferrite is the soft phase and its hardness is dependent on the alloying elements and the crystal defects.

Analyzing ESEM images with ImageJ was found to give an approximate result for this microstructure. The similar colors of the pearlite, Pb inclusions and grain boundaries made it difficult to adjust the threshold, leading to either counting everything as pearlite or to sacrificing some of the pearlite while leaving the grain boundaries and the Pb inclusions out of the selection. A total area of 8,67 mm² was analyzed to discover 9.1% of pearlite.

ImageJ analysis of LOM images revealed the area percentage of pearlite together with the inclusions to be 12.57%. Subtracting the 1.8% of inclusions, that were calculated earlier from the ESEM images, results in 10.77% of pearlite.

By using the pixel replacement method, it was found that the average area percentage of pearlite is 10.56%, the number being very close to the second method discussed above with a difference of just 0.21%. Having this amount of pearlite in steels is very common. The use of either of the last two methods is believed to be efficient in the calculation of the pearlite area. Python has been used just to bring an example of how programming software can be used for solving this problem, but there are many other alternatives that can do the same job.

3.1.2 Inclusions

The inclusions results should be treated as an approximation when related to the whole material batch as the microscopic examination can accurately describe only the analyzed area. In reality, it is very common for inclusions to vary in shape and size from billet to billet even within the same batch.

Different elements appear on the image as brighter or darker regions depending on their mean atomic number (Z), a larger atomic number giving a brighter appearance. The total imaged area represented by 26 images on each sample is 6.8 mm². As can be seen from the micrograph in Figure 7 (left), the inclusions are evenly distributed, have an elongated shape (spindle-shaped) and vary in size. The steel bars are obtained by hot rolling of ingots, this causes the inclusions to elongate in the rolling direction. Some of the inclusions are compound and have different constituents.

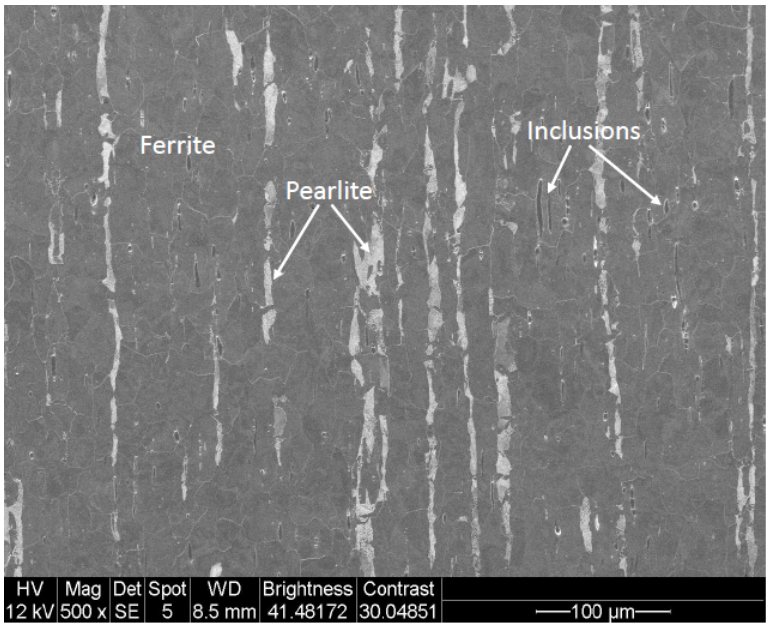

a) ESEM micrograph

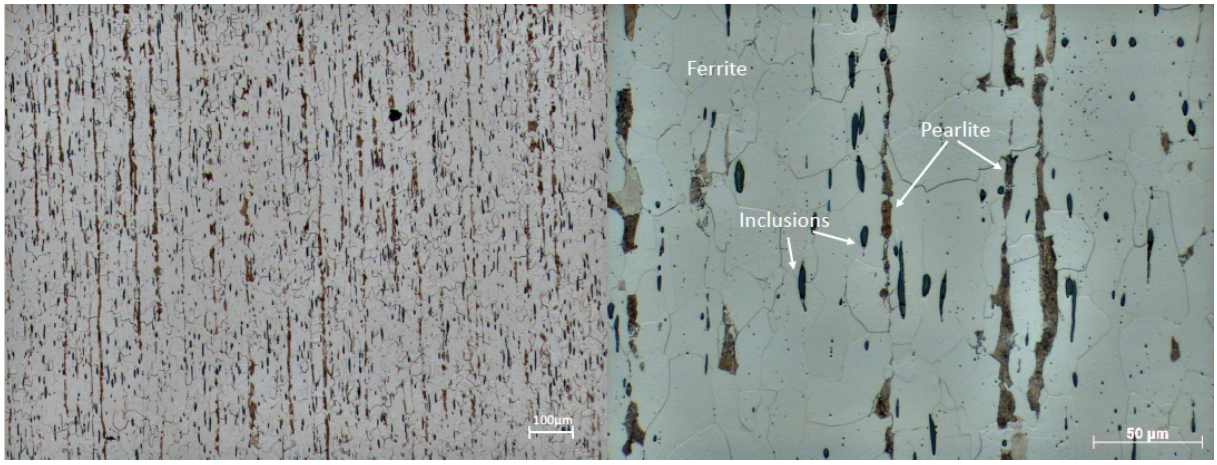

b) LOM micrographs

Figure 6: Free-cutting steel micrographs

The study of results revealed the presence of MnS and Pb inclusions. The micrograph in Figure 7 (right) shows that MnS and Pb inclusions exist as separate entities and as a combination of both. In the combined inclusions, Pb appears to be at the tapered edges of the spindle shape most of the times. A very low amount of oxide in the form of black color stripes and dots was spotted in some of the inclusions.

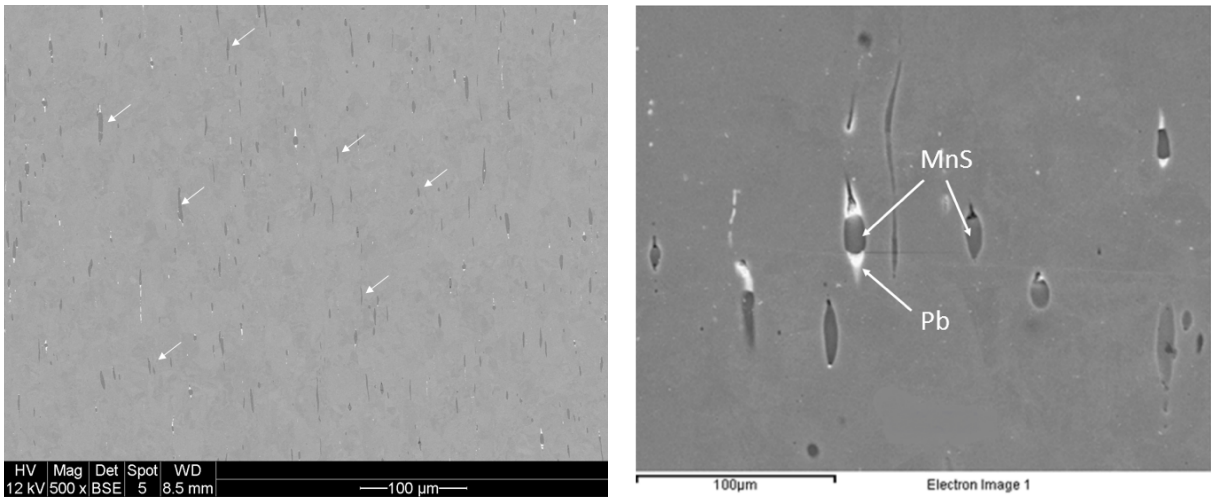

Figure 7: Inclusions micrographs

Table 4 summarizes the calculated values for area percentage, total area and the average size averaged over 26 images. One of the main tasks in inclusions analysis was to determine if there is any difference in shape, size or distribution on the two planes at a 90˚ angle in the rolling direction of the material. As shown in Table 4, the average size of the inclusions varies significantly but the total area percentage is almost the same. This shows that there is no major difference in the inclusions distribution but there is some disparity in the size, a possible rolling effect.

		% Area	Total Area (µm²)	Average size (µm²)
Sample 1	Pb	0.22	536.09	1.63
	MnS	1.41	3461.30	14.62
Sample 2	Pb	0.21	519.81	0.71
	MnS	1.59	3846.06	9.56

Table 4: Inclusions results

A graphical representation of the Mn and Pb inclusions' area percentage is shown in Figure 8. The difference between the inclusions in perpendicular directions is insignificant and thus the samples will be regarded as being the same in terms of inclusion content.

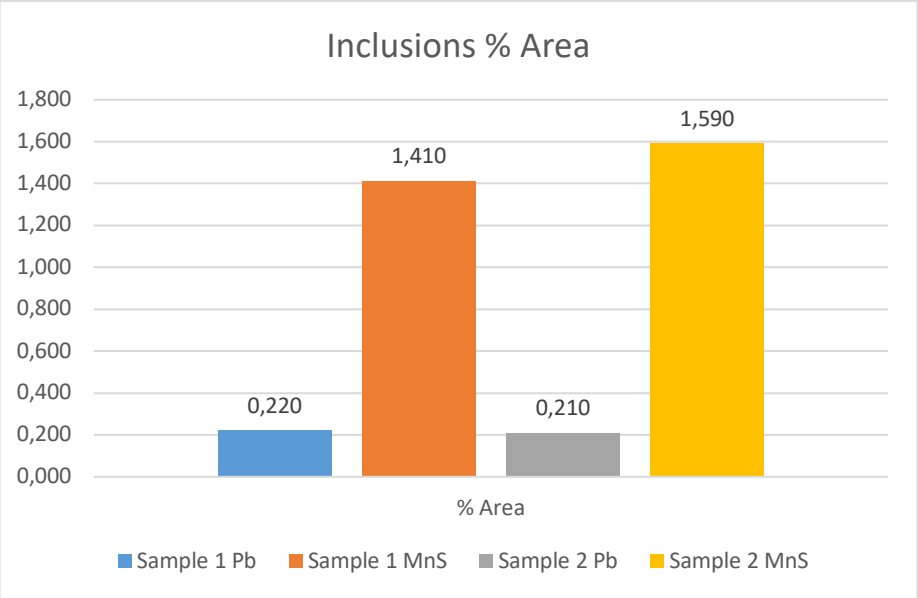

Figure 8: Inclusions area percentage

3.1.3 Hardness

The average hardness values along the rod diameter showed no significant difference between the two sets of data points: 196.9 HV for the first row and 198.7 HV for the second row. This makes 197.8 HV be the representative hardness value for the tested specimen with a standard deviation of 7.6 HV. The larger differences between some of the hardness values are due to the indenter heating different phases which vary in hardness.

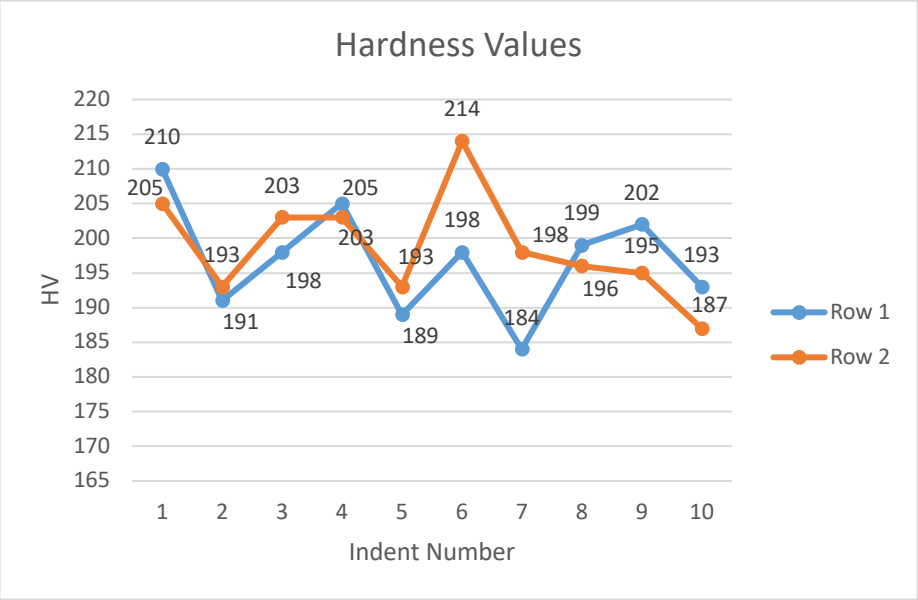

Figure 9: Vickers hardness values

3.2 Machined Surface Roughness

As depicted in Figure 10, changing the cutting fluid did not have a significant impact on the surface finish of the machined components (also see Figure 22, 23). The Ra value, when machining with mineral oil, varies between 2.357 µm and 2.899 µm with a standard deviation of 0.102 µm. Machining with neat vegetable oil resulted in an Ra value between 2.397 µm and 2.719 µm with a standard deviation of 0.089 µm. It is important to note that even though switching to vegetable oil did not bring a major improvement to the surface roughness, it did not worsen it either and thus should be considered as a replacement for the mineral oil due to other numerous benefits it has. The minor difference in the surface roughness might be an effect of the difference in the BUE and the variation of cutting fluids. A larger BUE on the tool causes the adhered material to smear on the workpiece surface.

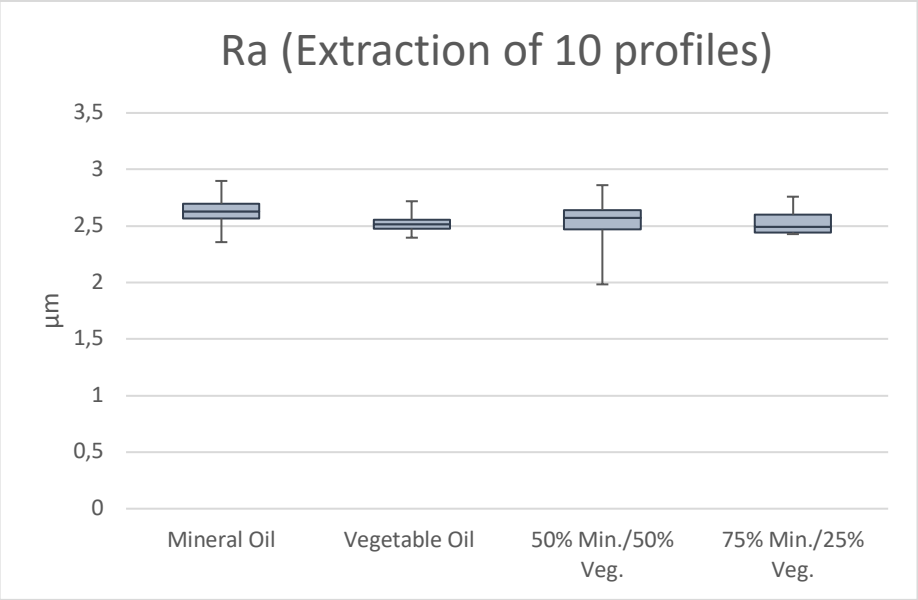

Figure 10: Surface roughness (Ra)

Similarly, it was attempted to determine if the surface roughness would be lower when machining with a new tool than with a worn tool. Thus, the surfaces of the first and the last machined parts for each tool have been analyzed. The results showed no consistency with this prediction, in fact for some components, the surface roughness was better when machining with a worn tool. A possible reason for this could be the constantly changing microgeometry of the insert nose as the adhered BUE grows and falls off.

3.3 Tool Wear

Four drill bits have been analyzed in order to determine their substrate and coating composition as well as the predominant tool wear mechanisms. The flank wear has been measured on each of the drill bits and the variation is depicted in Figure 12. One extra drill bit used with mineral oil has been supplied for analysis but was not a part of the machining test. Even though the number of machined components for this drill bit was

significantly higher, the flank wear did not change much (the mineral oil bar on the left, Figure 12).

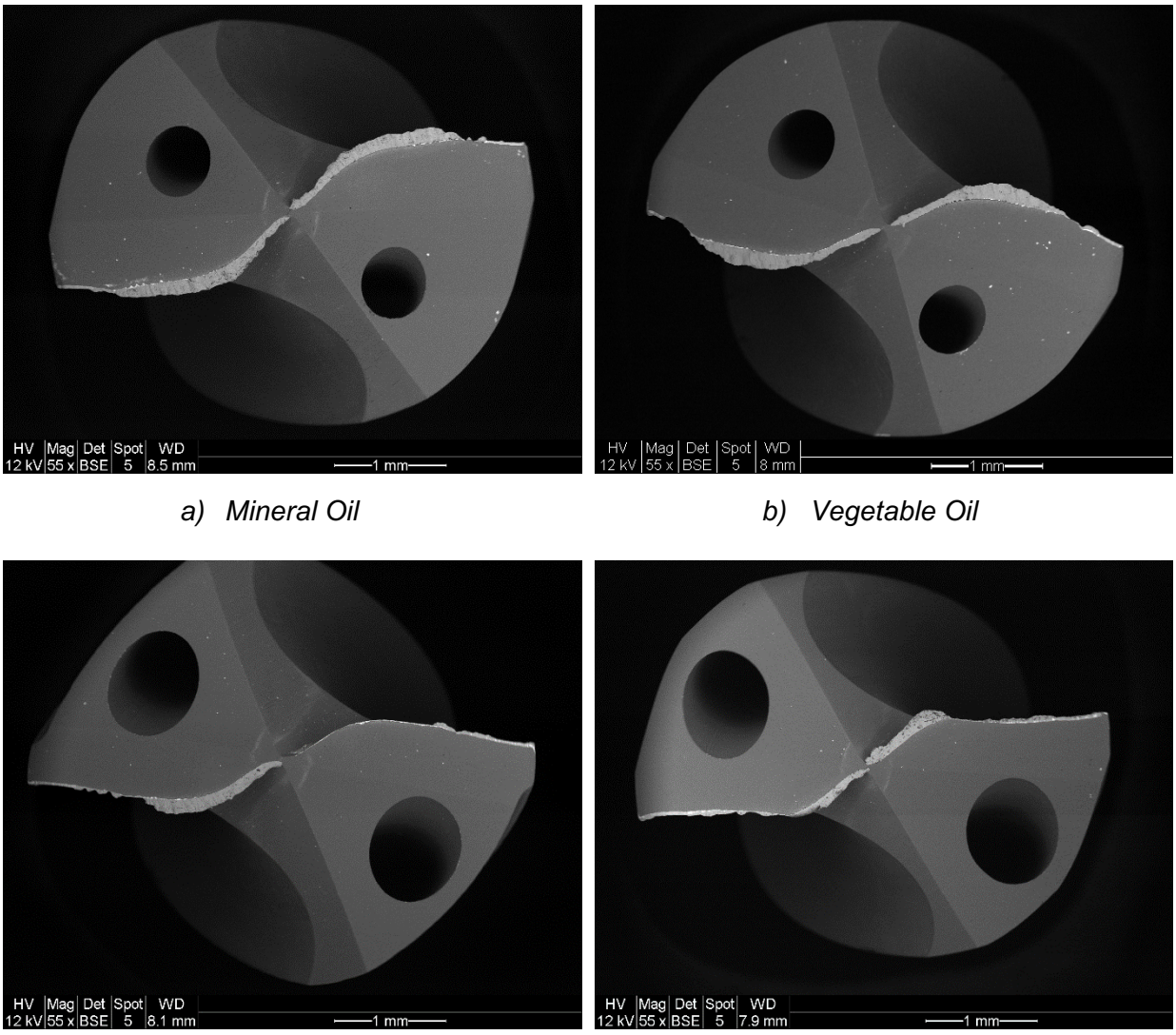

a) Mineral Oil *b) Vegetable Oil*

c) 50% Mineral Oil - 50% Vegetable Oil *d) 75% Mineral Oil - 25% Vegetable Oil*

Figure 11: ESEM micrographs of drill bits after machining with different cutting fluids

The best cutting performance was obtained using mineral oil, followed by the 50% - 50% mixture, vegetable oil and the mixture of 25% vegetable - 75% mineral oils. It is unknown whether repeating the same test several times would result in a similar output. The drill bits are reground and recoated and thus can vary in the cutting edge geometry as it can be observed from Figure 11.

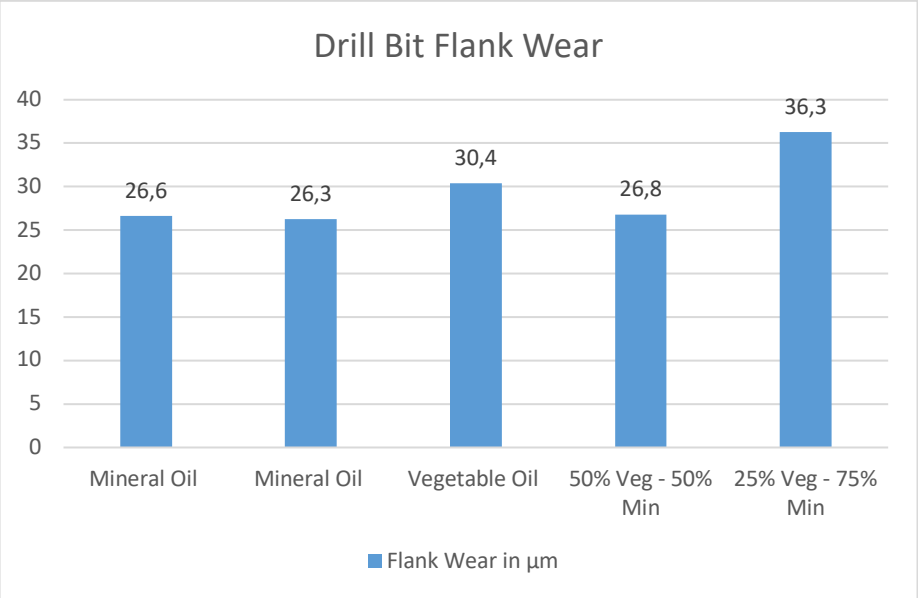

Figure 12: Drill bits flank wear measurements

Chipping of the cutting edge has been observed for the drill bit used with vegetable oil. The BUE appears to be larger in cases where a single oil has been used and smaller when machining with a mixture of the two oils. The BUE is a material deposit on the rake face of the tool that locally prevents the direct contact between the tool tip and the overflowing chips. It also changes the tool geometry and reduces the contact area leading to lower cutting forces, temperatures and power consumption. As discussed by Trent (“Metal Cutting”, 2000), the BUE easily resists cutting forces and can have a hardness of up to 700 HV. It is more likely to appear in steel at low cutting speeds, decreasing as the cutting speed increases, and largely depends on the feed rate. There is a critical cutting speed after which BUE does not form anymore. The reason for this is that higher cutting speeds lead to higher temperatures that cause the pearlite in the material to undergo recovery and crystallization, significantly decreasing the ability of BUE to resist stresses, and eventually transforming it into a flow zone. A large BUE can negatively affect the surface roughness of the machined components, while a small BUE (<= feed) is known to facilitate the sulfide deposition on the tool surface and does not have as much effect on the surface quality.

It was determined that the drill bits have a WC-Co substrate and are coated with (Al,Cr)N (see Figure 24 and 25). As shown by the elemental mappings, the BUE mostly consists of iron from the workpiece material.

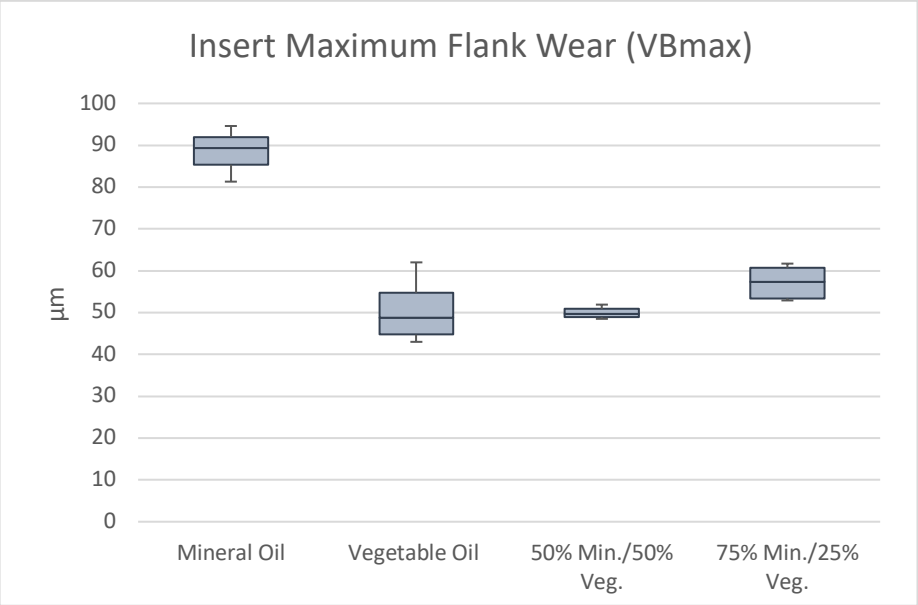

Figure 13: Insert maximum flank wear measurements

The flank wear measurements on the cutting inserts are depicted in Figure 13. As the volume percentage of mineral oil in the cutting fluid decreases, the flank wear also decreases. While there is an abrupt change in the flank wear between machining with pure mineral oil and a mixture, the flank wear does not change as much when switching from machining with a mixture of oils to machining with pure vegetable oil. Thus, it might not be economical for a company to substitute all the mineral oil used in the machining at once. Gradually replacing the mineral oil by vegetable oil, as it is consumed/worn out, would not only cut the expenses but also eliminate the need to dispose of the mineral oil. Figure 14 illustrates the differences in the flank wear of two carbide inserts used in turning operations with the same cutting parameters but with different cutting fluids, 100% mineral oil and 50% mineral - 50% vegetable oils (see also Figure 26). The flank wear appears to be uniform along the depth of cut but has a maximum wear spot close to the nose radius. This could be caused by the local stresses that were the highest at that spot. Using EDS allowed to identify the microstructural components on the inserts (Figure 28-30). The inserts are coated with TiCN by PVD. The sheared material and overflowing chips cause the coating on the tool to wear out and expose the substrate. Similarly, when the BUE reaches a critical size, it can rupture and carry away with it a part of the coating, thus exposing the substrate. Having a higher hardness, the carried away coating particle can cause abrasion on the tool surface. This combined effect of adhesion and abrasion is called attrition wear. The bright regions on the wear land represent the exposed WC-Co tool substrate where Co acts as a binder. Most of the wear happens around the insert nose where the BUE formation is predominant.

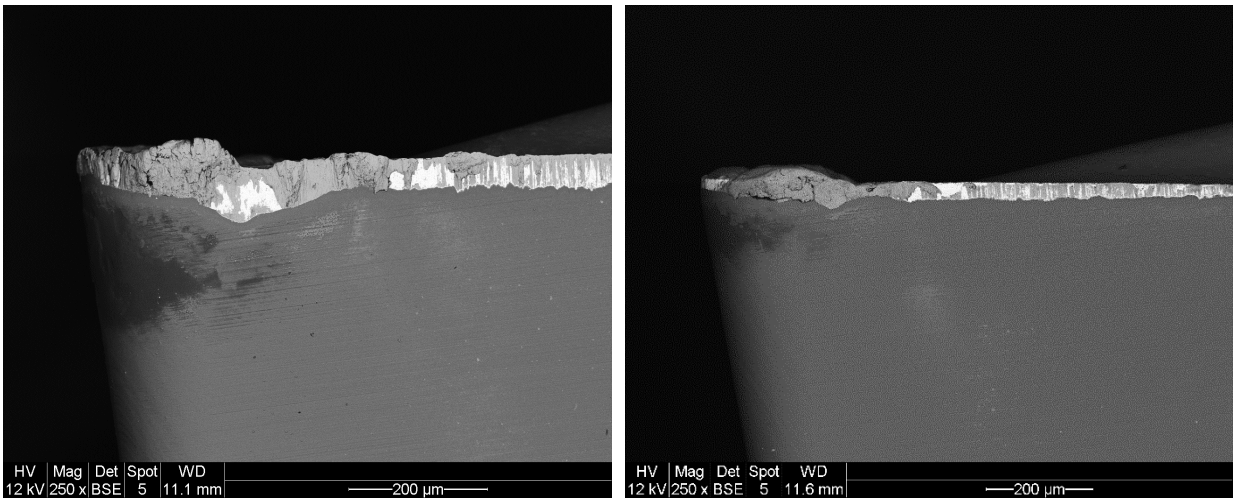

Figure 14: Insert flank wear with 100% mineral oil (left) and 50% mineral – 50% vegetable oils (right)

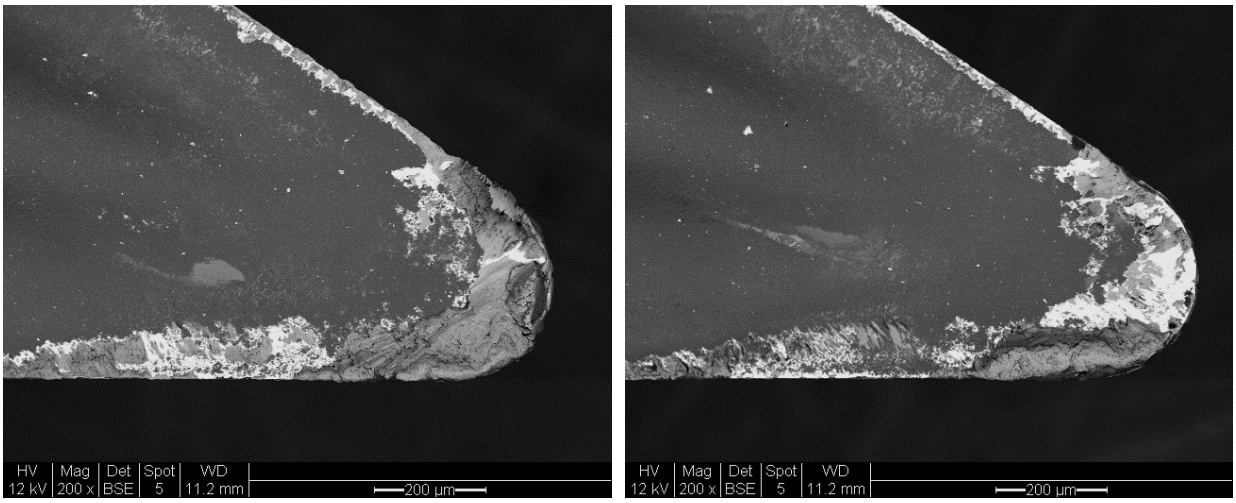

Figure 15: Insert wear on the rake face with 100% mineral oil (left) and 100% vegetable oil (right)

Turning FCSs at comparatively low cutting speeds results in the formation of discontinuous chips. This is a positive aspect considering that the chips are not long enough to cause wrapping around the tool or damage the workpiece surface as it happens with the continuous chips. The friction between the workpiece and the tool causes material to adhere to the tool surface. Being pushed by new material in the shear plane, the adhered material is forced to bulge out and crack forming a chip.

It was noted that a BUE is more likely to form on the substrate as the coating on the tool prevents material adhesion. It is common for crater wear to originate at low and medium cutting speeds when machining leaded steels with WC-Co tools. Absence of this type of wear can be due to the effectiveness of the coating in the tested inserts or the ability of the adhered material to prevent further wear of the substrate. Figure 15 illustrates the wear on the rake faces of two carbide inserts used in turning operations with neat mineral and vegetable oils (see also Figure 27). The BUE is significantly lower

in the case of machining with vegetable oil, adhesion wear being the predominant wear mechanism in all the examined tools.

During the machining of FCSs, a thin layer of MnS is formed on the tool surface and can cover both flank and rake faces. Such a layer has lubricating properties and prevents direct contact between the tool and the workpiece material. Its presence on all of the rake faces of the analyzed inserts was confirmed by the EDS analysis. As seen from Figure 15, 27 and 29, the sulfide layers formed far away from the cutting edge, rarely appearing on the contact area between the tool and the workpiece (happens at very low cutting speeds). MnS layers are believed to significantly reduce the diffusion wear and the BUE formation, possibly due to a lower temperature at the location of these layers.

3.4 Oil Purity and Viscosity

The purity test results were inconclusive as the number of particles was too high to count. This could be due to a faulty filtering system in the CNC, a wrong sampling location or the high amount of build-up dirt that was stirred up during the oil change.

	Aimed Mixture	Actual Mixture	Viscosity (cSt)
Week 1 - start	100% Mineral Oil	100% Mineral Oil	21.7
Week 1 - end			21.8
Week 2 – start	100% Vegetable Oil	100% Vegetable Oil	11.1
Week 2 - end			11.2
Week 3 – start	50% Min. + 50% Veg.	35% Min. + 65% Veg.	14.0
Week 3 - end			14.0
Week 4 – start	75% Min. + 25% Veg.	55% Min. + 45% Veg.	15.9
Week 4 - end			15.9

Table 5: Oil mixtures and their viscosities

None of the cutting fluids represented in Table 5 had shown a change in viscosity from the beginning to the end of the week as for neat oils this testing time is too short to observe any changes in their properties. It was found that the actual volumes of each oil in the mixtures were different from the intended ones. Thus, instead of having 50% mineral and 50% vegetable oils in the machining process, a mixture of 35% mineral and 65% vegetable oils has been used. Similarly, 75% - 25% proportion turned out to be 55% - 45%. The inability to completely drain the cutting fluids from the system has probably caused these differences in the volume fractions. Another possibility is that the two oils could not form a uniform blend before sampling resulting in different, from the ones intended, proportions inside the sample container and not necessarily in the CNC. The viscosity of the mineral oil has been reported to be 21.7 cSt, this value being the most reliable as it represents the oil that was in the system before any changes in the cutting fluid occurred. The vegetable oil used has a lower viscosity of 11.1 cSt and this might have positively affected the heat removal from the cutting zone. Likewise, using a lower viscosity oil can result in better chip-removing ability.

4. Conclusions

The metal cutting fluids used in the industry are raising concerns about sustainability, biodegradability and the associated health risks. Numerous studies show the benefits of using vegetable oil-based MCFs. This study focused on determining the influence of different cutting fluids on the workpiece morphology and tool wear. The case is about carbide inserts and drill bits used in turning and drilling operations performed on free-cutting steel (FCS). The microstructure of the workpiece material was analyzed in an attempt to determine the role of the microstructural components in the machinability of FCSs. Ferrite, pearlite and MnS/Pb inclusions represent the microstructural constituents of the investigated FCS. No hardness variation within the raw material has been determined. The surface roughness of the machined components has not shown any dependence on the choice of cutting fluid.

The maximum flank wear measurements on the carbide inserts appear to follow a trend where increasing the amount of vegetable oil in the mixture leads to a reduction in tool wear. This result was sought-after due to the many benefits that the vegetable oil has as a cutting fluid. Adhesion and BUE formation are the predominant wear mechanisms for both of the tool types. The flank wear measurements on the drill bits showed that the best machining performance can be achieved by using mineral oil, followed by the mixture of 50% mineral – 50% vegetable oils, vegetable oil and the mixture of 75% mineral – 25% vegetable oils. This result cannot be decisive in whether a cutting fluid had an influence on this tool wear behavior and thus should not be considered. The reason for this is a low number of drill bit samples available for analysis and the fact that the drill bits did not reach the end of their tool life.

Nevertheless, the objective of this master's thesis to identify the tool wear behavior under the influence of the tested cutting fluids was accomplished. Based on the tool wear analysis of the carbide inserts, the vegetable oil has performed similar or better than the conventional mineral oil in all the aspects and thus should be considered as a sustainable alternative.

Further research needs to be done in order to evaluate all the possible variations that come with the change of the cutting fluid. The cutting forces and temperatures at the contact point between the tool and the workpiece could vary and differently affect the tool wear and the surface roughness of the machined components. The nature and contribution of the oxide found in the microstructure remains to be determined. This study attempted to find a way to define the amount of each of the constituents, and thus its findings could be further developed and used to characterize the influence of batch to batch variations on tool wear when machining with different cutting fluids. Surface roughness measurements after the drilling operations could determine how the cutting fluids affect the drilled surface quality. Testing a larger number of samples generates a more reliable data set. The use of new drill bits in the future could eliminate the cutting edge geometry variations and permit a more thorough wear investigation. Oil mixability tests are required in order to understand how to locally control a constant volume of different oils in a mixture, improve oil sampling methods and find a more precise way to mix different oils. The long-term performance of the vegetable oil is unknown and should be investigated.

Bibliography

- Abdalla, H. S., Baines, W., Mcintyre, G., & Slade, C. (2006). Development of novel sustainable neat-oil metal working fluids for stainless steel and titanium alloy machining. Part 1. Formulation development. *The International Journal of Advanced Manufacturing Technology*, *34*(1-2), 21–33. doi: 10.1007/s00170-006-0585-4.

- An, Q., Liu, Z., Jiang, L., & Chen, M. (2014). Experimental and numerical research on the effects of minimum quantity lubrication in thread turning of free-cutting steel AISI 1215. *Proceedings of the Institution of Mechanical Engineers, Part B: Journal of Engineering Manufacture,229*(5), 878-885. doi:10.1177/0954405414534429.

- Ånmark, N., Karasev, A., & Jönsson, P. (2015). The Effect of Different Non-Metallic Inclusions on the Machinability of Steels. *Materials,8*(2), 751-783. doi:10.3390/ma8020751.

- Belluco, W., & Chiffre, L. D. (2004). Performance evaluation of vegetable-based oils in drilling austenitic stainless steel. *Journal of Materials Processing Technology,148*(2), 171-176. doi:10.1016/s0924-0136(03)00679-4.

- Bhowmik, P., Kumar, U., & Arora, G. (2015). Vegetable oil based cutting fluids-green and sustainable machining – I. Journal of Material Science and Mechanical Engineering,2(9), 1-5.

- Chiffre, L. D., & Belluco, W. (2000). Comparison of Methods for Cutting Fluid Performance Testing. *CIRP Annals,49*(1), 57-60. doi:10.1016/s0007-8506(07)62895-9.

- Davim, J. P., Gaitonde, V., & Karnik, S. (2008). Investigations into the effect of cutting conditions on surface roughness in turning of free machining steel by ANN models. *Journal of Materials Processing Technology,205*(1-3), 16-23. doi:10.1016/j.jmatprotec.2007.11.082.

- De Chiffre L. Investigations of Cutting fluid performance using different machining operations. Lubr Eng 2002:22-8.

- Debnath, S., Reddy, M. M., & Yi, Q. S. (2016). Influence of cutting fluid conditions and cutting parameters on surface roughness and tool wear in turning process using Taguchi method. *Measurement,78*, 111-119. doi:10.1016/j.measurement.2015.09.011.

- *Exploring surface texture: A fundamental guide to the measurement of surface finish*. (2011). Leicester: Taylor Hobson Limited.

- Fang, X., & Zhang, D. (1996). An investigation of adhering layer formation during tool wear progression in turning of free-cutting stainless steel. *Wear,197*(1-2), 169-178. doi:10.1016/0043-1648(96)06924-4.

- Gajrani, K. K., & Sankar, M. R. (2017). Past and Current Status of Eco-Friendly Vegetable Oil Based Metal Cutting Fluids. *Materials Today: Proceedings,4*(2), 3786-3795. doi:10.1016/j.matpr.2017.02.275.

- Geels, K. (2007). *Metallographic and materialographic specimen preparation, light microscopy, image analysis, and hardness testing*. Place of publication not identified: ASTM International.

- Gu, J., Barber, G., Tung, S., & Gu, R. (1999). Tool life and wear mechanism of uncoated and coated milling inserts. *Wear,225-229*, 273-284. doi:10.1016/s0043-1648(99)00074-5.

- Hazra, J., Caffarrelli, D., & Ramalingam, S. (1974). Free Machining Steels—The Behavior of Type I MnS Inclusions in Machining. *Journal of Engineering for Industry,96*(4), 1230. doi:10.1115/1.3438500.

- Hoier, P., Malakizadi, A., Klement, U., & Krajnik, P. (2019). Characterization of abrasion- and dissolution-induced tool wear in machining. *Wear,426-427*, 1548-1562. doi:10.1016/j.wear.2018.12.015.

- John, J., Bhattacharya, M., & Raynor, P. C. (2004). Emulsions containing vegetable oils for cutting fluid application. *Colloids and Surfaces A: Physicochemical and Engineering Aspects,237*(1-3), 141-150. doi:10.1016/j.colsurfa.2003.12.029.

- Junior, A. B., Diniz, A. E., & Filho, F. T. (2008). Tool wear and tool life in end milling of 15–5 PH stainless steel under different cooling and lubrication conditions. *The International Journal of Advanced Manufacturing Technology,43*(7-8), 756-764. doi:10.1007/s00170-008-1744-6.

- Khan, M. M., & Dhar, N. R. (2006). Performance evaluation of minimum quantity lubrication by vegetable oil in terms of cutting force, cutting zone temperature, tool wear, job dimension and surface finish in turning AISI-1060 steel. *Journal of Zhejiang University-SCIENCE A,7*(11), 1790-1799. doi:10.1631/jzus.2006.a1790.

- Khan, M., Mithu, M., & Dhar, N. (2009). Effects of minimum quantity lubrication on turning AISI 9310 alloy steel using vegetable oil-based cutting fluid. *Journal of Materials Processing Technology,209*(15-16), 5573-5583. doi:10.1016/j.jmatprotec.2009.05.014.

- Kolawole, S., K., & Odusote, J., K. (2013). Performance evaluation of vegetable oil-based cutting fluids in mild steel machining. Chemistry and Materials Research, 3(9).

- Kurimoto, T., Barrow, G., & Davies, B. (1982). The Influence of Aqueous Fluids on the Wear Characteristics and Life of Carbide Cutting Tools. *CIRP Annals,31*(1), 19-23. doi:10.1016/s0007-8506(07)63261-2.

- Laizhu, J., Kun, C., & Hänninen, H. (1996). Effects of the composition, shape factor and area fraction of sulfide inclusions on the machinability of re-sulfurized free-machining steel. *Journal of Materials Processing Technology,58*(2-3), 160-165. doi:10.1016/0924-0136(95)02144-2.

- Lawal, S., Choudhury, I., & Nukman, Y. (2012). Application of vegetable oil-based metalworking fluids in machining ferrous metals—A review. *International Journal of Machine Tools and Manufacture,52*(1), 1-12. doi:10.1016/j.ijmachtools.2011.09.003.

- M. Hashimura, A. Mizuno, K. Miyanishi, (2009). Effect of MnS Distribution on Machinability in Low-Carbon Free-Cutting Steel. *Iron & Steel Technology.*

- Malik, H., I., Mgaloblishvili, R., & Mills, B. (2000). Effect of TiN coating thickness on performance of HSS cutting tools when machining free cutting steels. Journal of Materials Science Letters, 19, 1779-1781.

- Ogedengbe, T. S., Awe, P., & Joseph, O. I. (2019). Comparative Analysis of Machining Stainless Steel using Soluble and Vegetable Oils as Cutting Fluids. *International Journal of Engineering Materials and Manufacture,4*(1), 33-40. doi:10.26776/ijemm.04.01.2019.05.

- Qin, C. J., Xia, M.Z., Ma, M.Y., & Zheng, Y.F. (2017). Effects of turning the microstructure on the mechanical properties and machinability of free-cutting steels. ASM International,26:3474-3481.

- Ramanujachar, K., & Subramanian, S. (1996). Micromechanisms of tool wear in machining free cutting steels. *Wear,197*(1-2), 45-55. doi:10.1016/0043-1648(95)06810-4.

- Shashidhara, Y., & Jayaram, S. (2010). Vegetable oils as a potential cutting fluid—An evolution. *Tribology International,43*(5-6), 1073-1081. doi:10.1016/j.triboint.2009.12.065.

- Siniawski, M. T., Saniei, N., Adhikari, B., & Doezema, L. A. (2007). Influence of fatty acid composition on the tribological performance of two vegetable-based lubricants. *Journal of Synthetic Lubrication*, *24*(2), 101–110. doi: 10.1002/jsl.32.

- *Standard Test Method for Microindentation Hardness of Materials*. (2010). West Conshohocken, PA: ASTM International.

- *Standard test method for Vickers hardness of metallic materials*. (2010). West Conshohocken, PA: ASTM International.

- *Standard test methods for determining the inclusion content of steel*. (2007). West Conshohocken, PA: ASTM International.

- Tamerabet, Y., Brioua, M., Tamerabet, M., & Khoualdi, S. (2018). Experimental Investigation on Tool Wear Behavior and Cutting Temperature during Dry Machining of Carbon Steel SAE 1030 Using KC810 and KC910 Coated Inserts. *Tribology in Industry,40*(1), 52-65. doi:10.24874/ti.2018.40.01.04.

- Tanaka, R., Yamane, Y., Sekiya, N. N., Sekiya, K., Narutaki, N., & Shiraga, T. (2007). Machinability of BN free-machining steel in turning. International Journal of Machine Tools and Manufacture,47, 1971-1977.

- Trent, E. M., & Wright, P. K. (2000). *Metal Cutting*. Butterworth-Heinemann.

- Wang, Y., Xie, F., Ma, S., & Dong, L. (2017). Review of surface profile measurement techniques based on optical interferometry. *Optics and Lasers in Engineering*, *93*, 164–170. doi: 10.1016/j.optlaseng.2017.02.004.

- Wang, Y., Yang, J., & Bao, Y. (2015). Effects of non-metallic inclusions on machinability of free-cutting steels investigated by nano-indentation measurements. The Minerals, Metals & Materials Society and ASM International. doi: 10.1007/s11661-014-2596-3.

- Xu, J., Liu, Z., Guo, G., & Chen., M. (2012). An investigation on wear mechanism of high-speed turning of free-cutting steel AISI 1215 using uncoated and multi-layer coated tools. Int J Adv Manuf Technol, 67:517-533. Doi: 10.1007/s00170-012-4502-8.

- Yaguchi, H. (1986). Effect of MnS inclusion size on machinabilty of low-carbon, leaded, resulfurized free-machining steel. *Journal of Applied Metalworking,4*(3), 214-225. doi:10.1007/bf02833929.

- Zhang, G., An, Q. L., Zhang, Y. S., Liu, G., & Chen, M. (2009). Study on the Machinability of Two Different Sulfur Free Cutting Steels. *Advanced Materials Research,69-70*, 510-514. doi:10.4028/www.scientific.net/amr.69-70.510.

Appendix A

Row	Diagonal 1	Diagonal 2	Diagonal (Avg.)	Hardness
Row 1	41.636	42.345	41.991	210
	43.558	44.462	44.01	191
	42.7	43.94	43.32	198
	42.168	42.877	42.522	205
	44.117	44.471	44.294	189
	42.877	43.585	43.231	198
	44.117	45.712	44.914	184
	43.208	43.131	43.169	199
	43.103	42.67	42.886	202
	44.14	43.421	43.781	193
Row 2	43.054	41.991	42.522	205
	43.94	43.766	43.853	193
	41.814	43.585	42.7	203
	43.763	41.814	42.788	203
	44.472	43.249	43.86	193
	41.817	41.469	41.643	214
	42.895	43.585	43.24	198
	44.312	42.703	43.507	196
	43.943	43.237	43.59	195
	43.799	45.357	44.578	187

Table 6: Vickers hardness test results

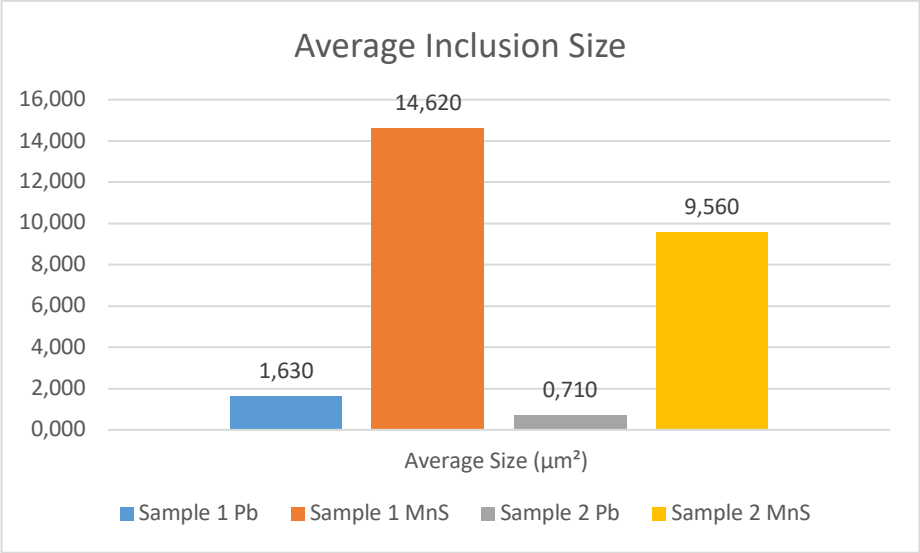

Figure 16: Average inclusion size (in the perpendicular directions)

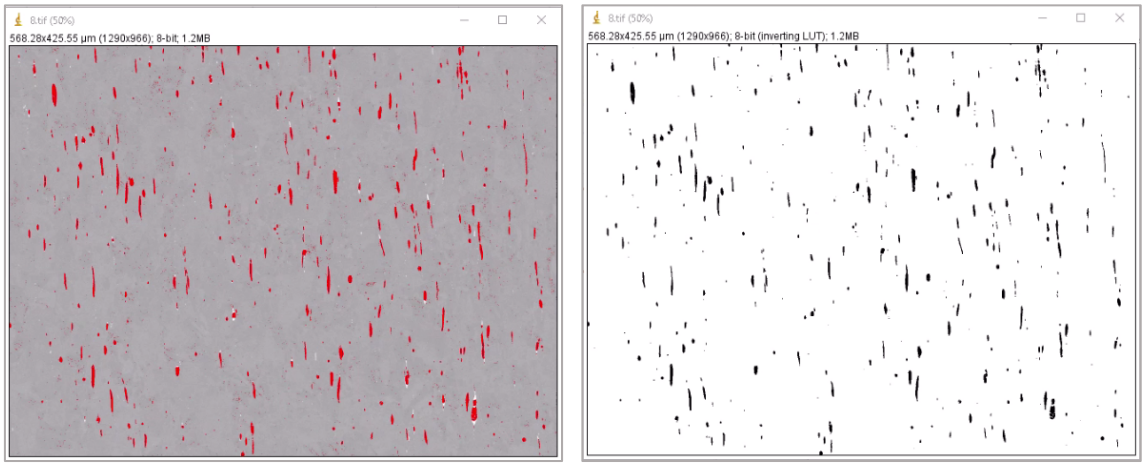

Figure 17: Threshold application in ImageJ (for MnS inclusions)

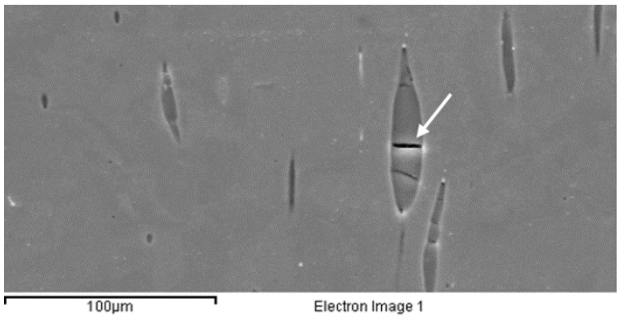

Figure 18: Micrograph showing the morphology of the oxide

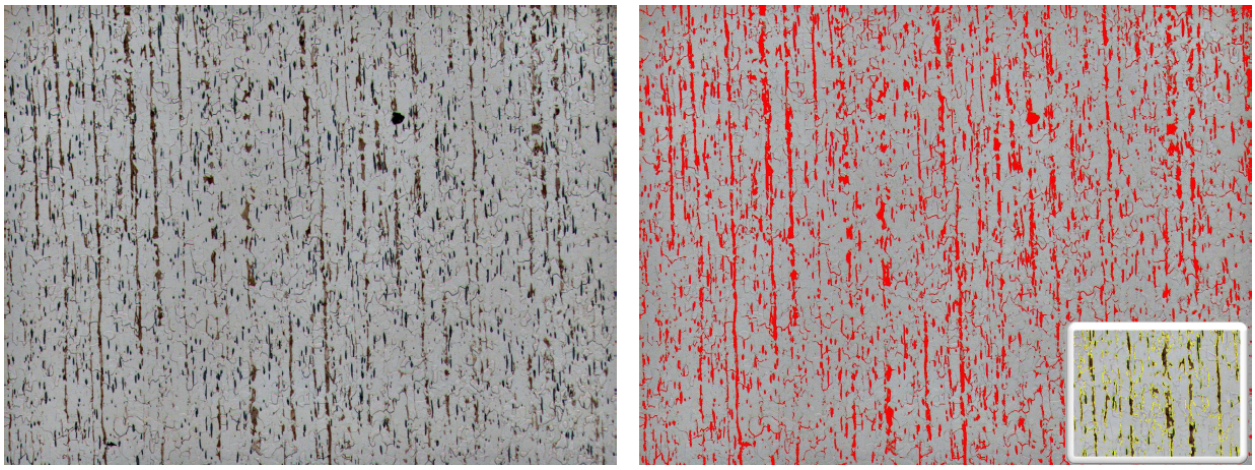

Figure 19: Applying threshold to LOM images

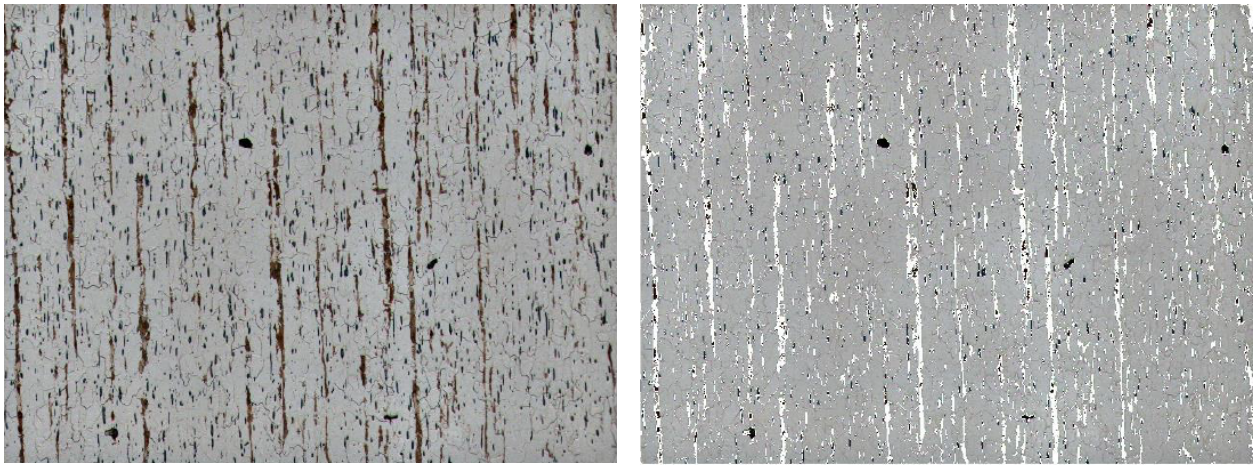

Figure 20: Pixel replacing process

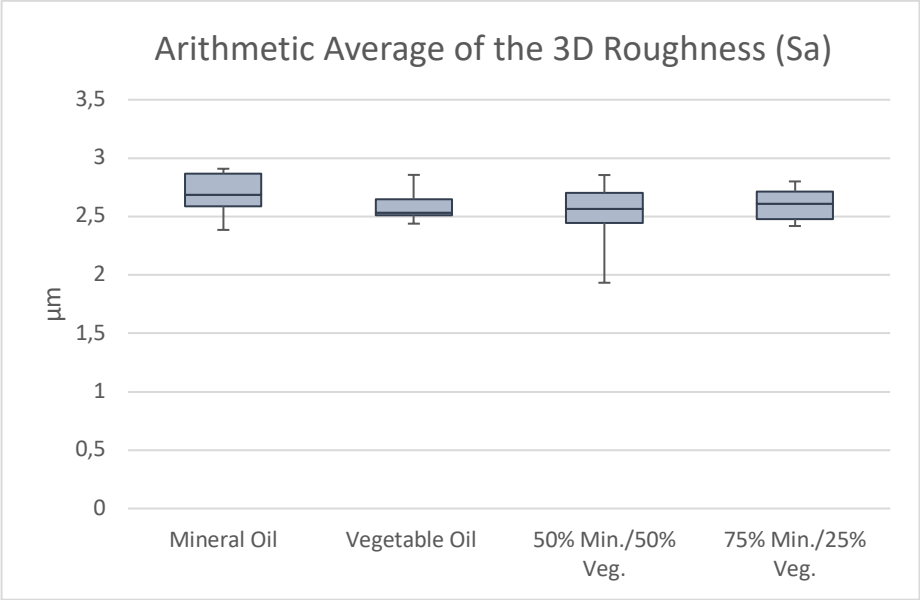

Figure 21: The arithmetic average of the 3D roughness

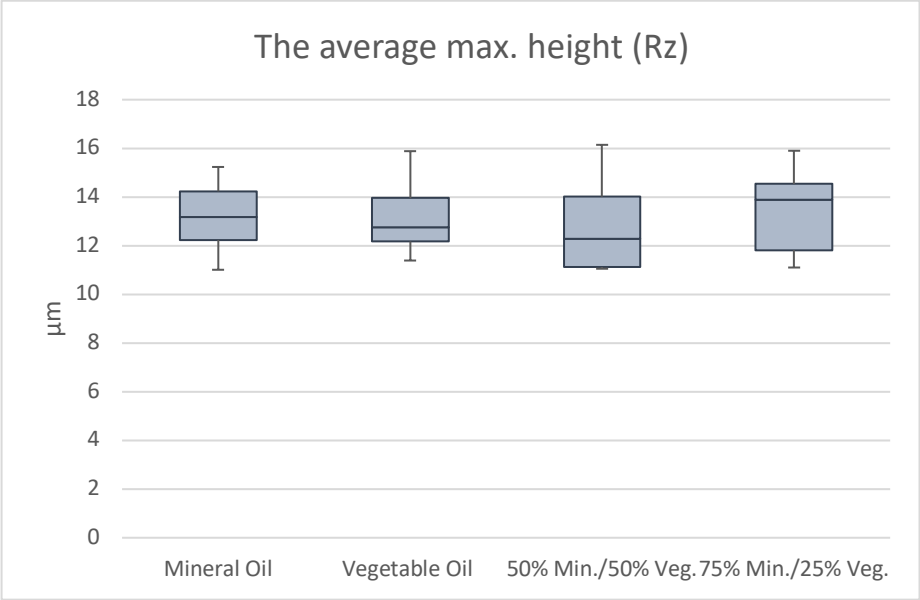

Figure 22: The average maximum height of the roughness profile (Rz)

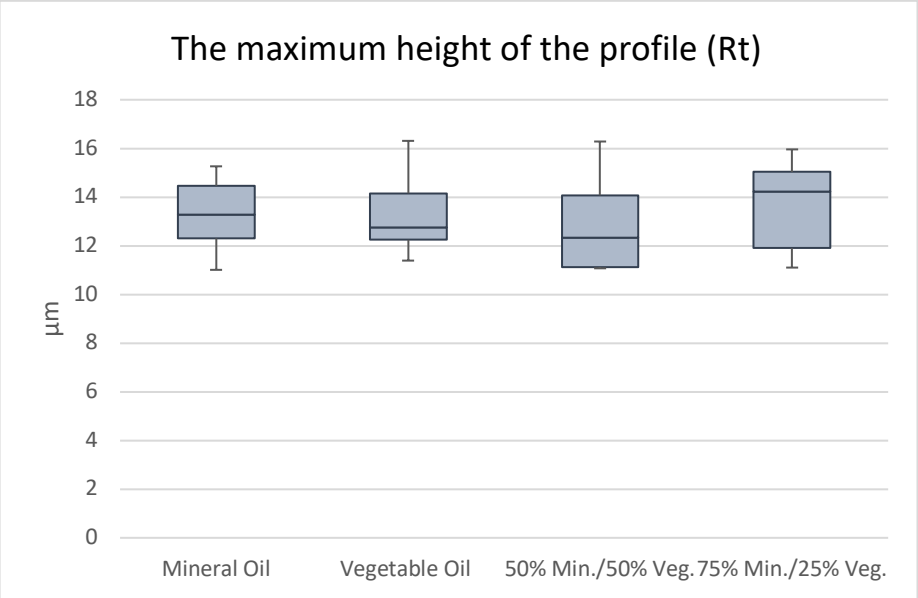

Figure 23: The maximum height of the roughness profile (Rt)

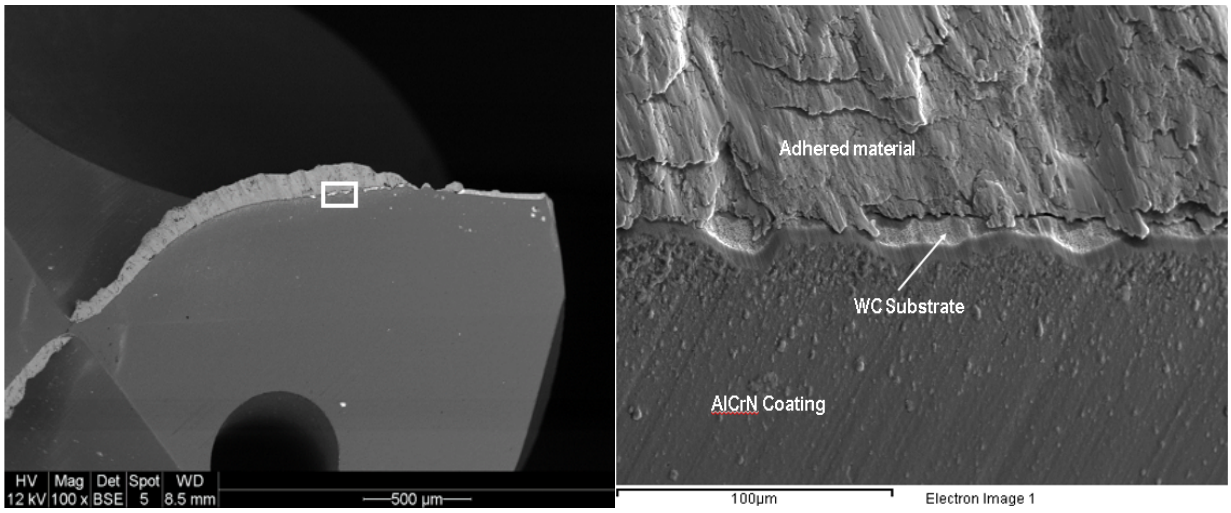

Figure 24: Drill bit flank wear

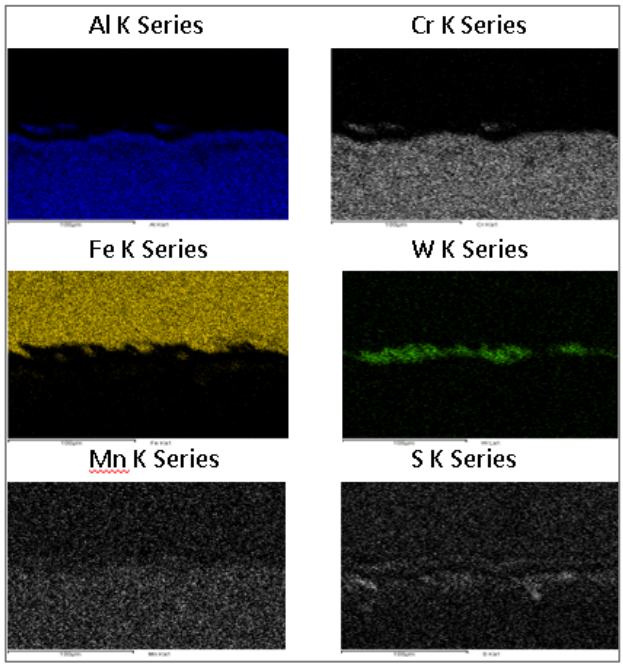

Figure 25: Elemental mapping on a drill bit (Figure 24 – right)

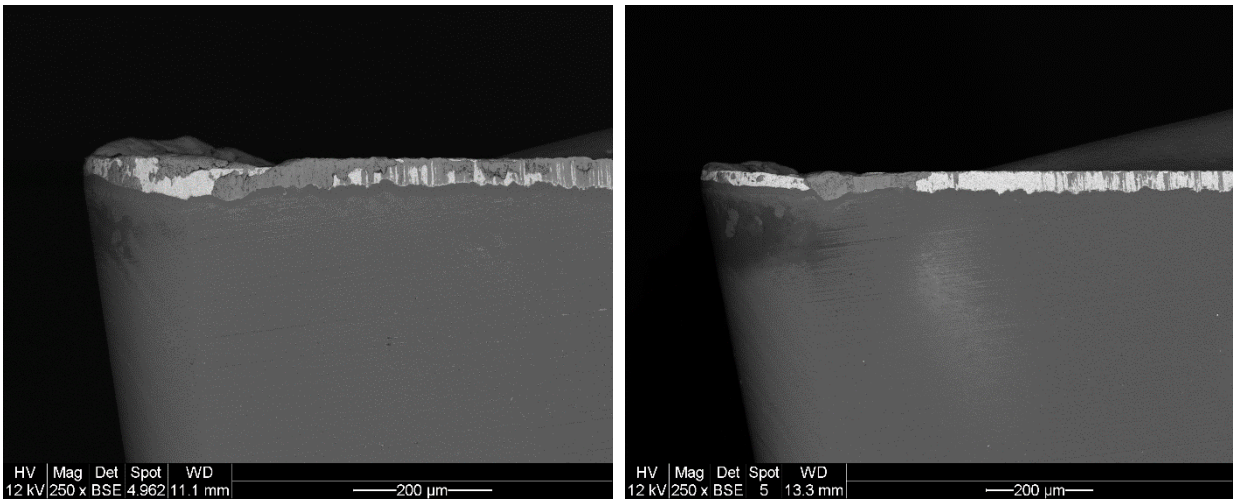

Figure 26: Flank wear with 100% vegetable oil (left) and 75% min. – 25% veg. oils (right)

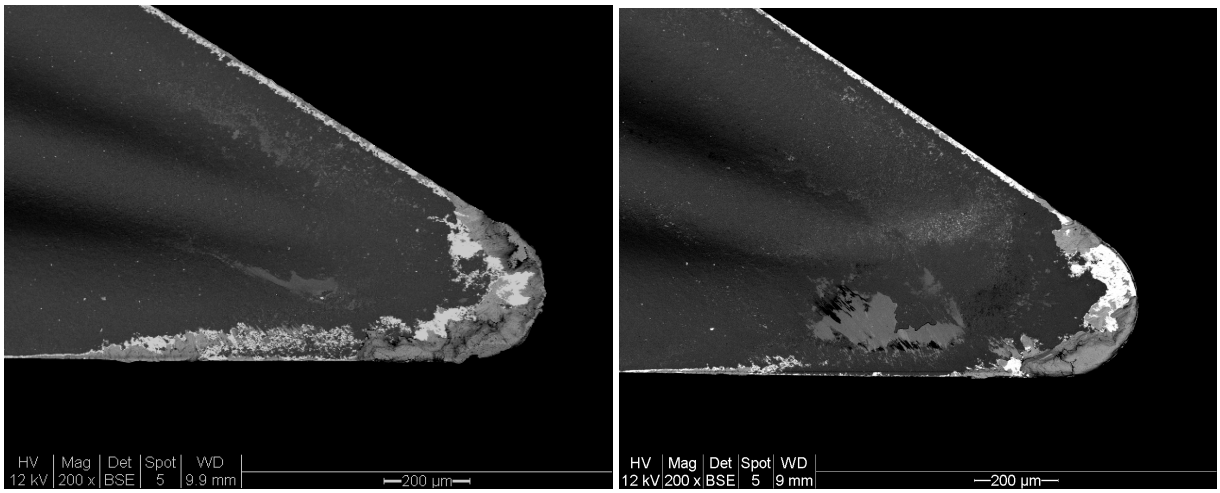

Figure 27: Insert wear on the rake face with 50% min. – 50% veg. oils (left) and 75% min. – 25% veg. oils (right)

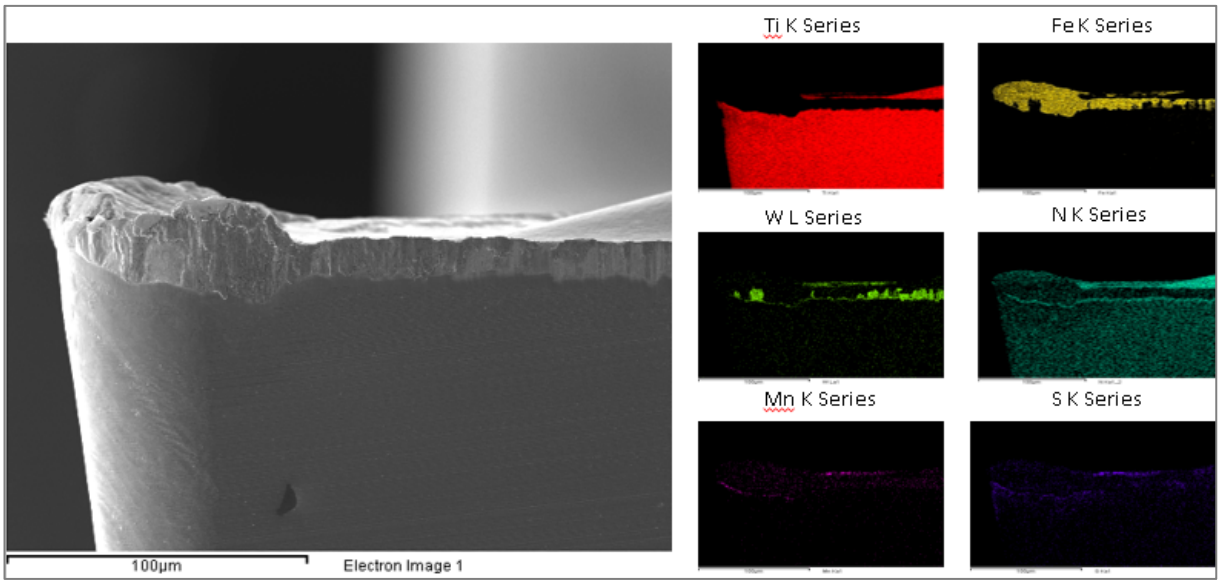

Figure 28: Elemental mapping of the insert flank face, 100% mineral oil

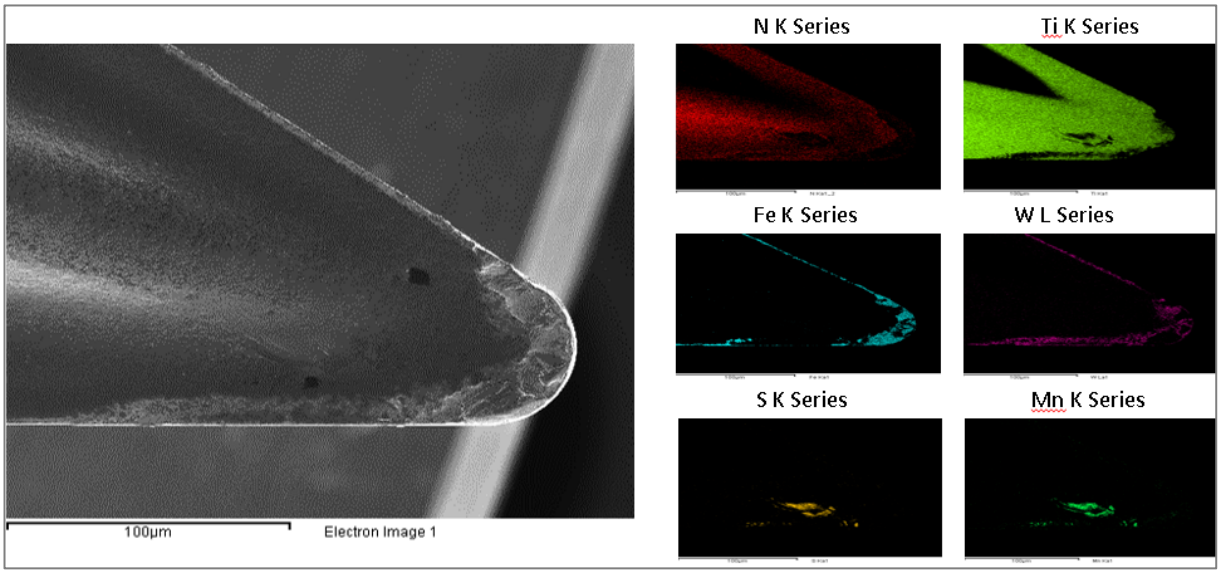

Figure 29: Elemental mapping of the insert rake face, 100% mineral oil

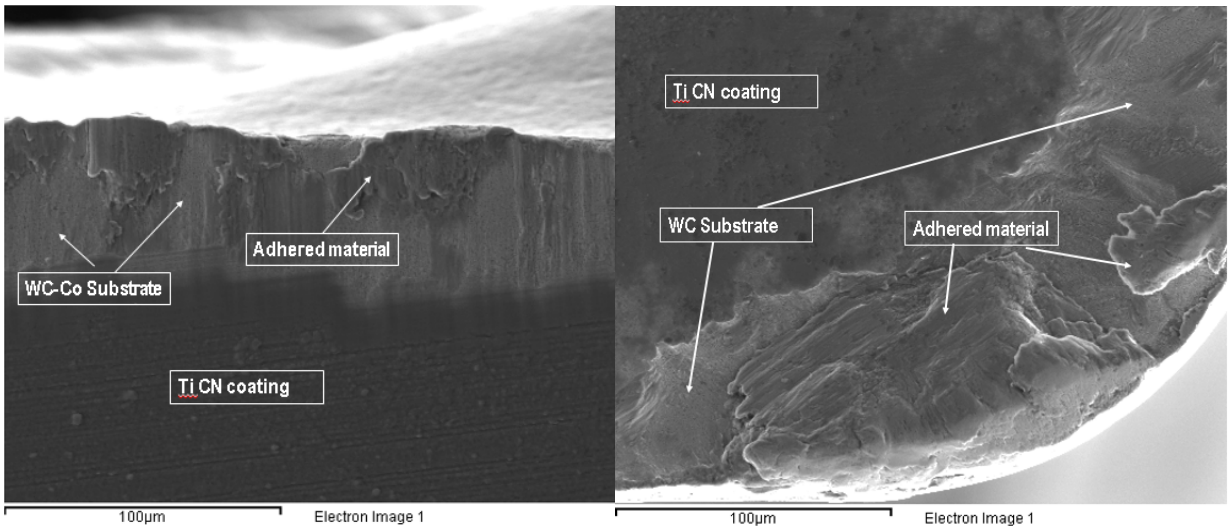

Figure 30: Insert wear on the flank (left) and on the rake (right) faces

Fluid Type	Edge #	Maximum Flank Wear (VBmax)
Mineral Oil	1	89.4 μm
	2	94.6 μm
	3	81.3 μm
Vegetable Oil	1	45.3 μm
	2	62 μm
	3	52.3 μm
	4	43 μm
50% Mineral Oil 50% Vegetable Oil	1	50.5 μm
	2	51.9 μm
	3	48.5 μm
	4	49 μm
75% Mineral Oil 25% Vegetable Oil	1	61.7 μm
	2	60.7 μm
	3	53.4 μm
	4	57.3 μm
	5	52.9 μm

Table 7: Maximum flank wear measurements for the carbide inserts

Pearlite Detection

```
import matplotlib.pyplot as plt
import numpy as np
import time

img = plt.imread("ImageName.jpg")
img_arr = img.reshape(-1, 3)
img_counted = img_arr.copy()

light_brown = (105, 80, 60)

num_l_brown = 0.0
bound = 45
l_bound = bound
u_bound = bound

for i, pix in enumerate(img_arr):
    r, g, b = light_brown
    if (r - l_bound) < pix[0] < (r + u_bound) and \
        (g - l_bound) < pix[1] < (g + u_bound) and \
        (b - l_bound) < pix[2] < (b + u_bound):
            img_counted[i] = np.array([255, 255, 255])
            num_l_brown += 1

percent = num_l_brown / np.shape(img_arr)[0] * 100

fig = plt.figure(figsize=(25, 10))
plt.axis('off')
plt.title(f"{percent:.2f}% masked")
fig.add_subplot(1, 2, 1)
plt.imshow(img)
plt.axis('off')
fig.add_subplot(1, 2, 2)
plt.imshow(img_counted.reshape(np.shape(img)))
plt.axis('off')
fig.axes[0].get_xaxis().set_visible(False)
fig.axes[0].get_yaxis().set_visible(False)
plt.savefig(f"img_{int(time.time())}.jpg")
plt.show()
```

Figure 31: Python code for pearlite detection